

UNIVERSITY OF HERTFORDSHIRE

SCHOOL OF PHYSICS, ASTRONOMY AND MATHEMATICS

---

# New Binary Systems in Gaia and their Properties

---

*Author:*  
Alok Singh

*Supervisor:*  
Prof. Hugh Jones  
*Co-Supervisor:*  
Prof. R.Smart

Project report submitted for the degree of

*MSc. Data Science*

## Abstract

In this investigation, 10702 GAIA EDR3 sources are used to identify binary systems. The binary systems must have a separation of less than 100 au[1] to have a minimum energy to be a bound system. They must also have a difference in parallaxes of less than 1.0 mas, and the difference in proper motion must be less than the 10% of the proper motion of primary source. In order to identify the age of systems, it is important to have a greater resolution on the colour magnitude diagram. In this project, the G-K magnitude is used instead of G-RP for colour magnitude H-R diagram to achieve greater resolution, due to which the objects with 2MASS K magnitude are used. This produces a list of 142 prospective binary systems. The most important feature of the binary system is that they have the same age. To estimate the age and the mass of the systems, the theoretical isochrone that contains all range of masses (mass  $> 0.01M_{\odot}$ ) along with G and K magnitude is used. After considering various models, the ATMO(BAHC15) is considered as the appropriate model to use because it contains low mass sources. This model also provides the most accurate evolutionary track of the sources with low masses and binary systems in comparison to other existing models.

The known objects are used to find the error in the absolute G and the G-K magnitude in order to identify empirical isochrones. The isochrones with age  $> 1.0$  Gyrs are difficult to identify due to the nature of the isochrones. The evolution takes place slowly as the age of the star increases. This means that the isochrones will lie very close to each other and may overlap with other ages. Therefore, it is difficult to differentiate between the ages between 1.0 Gyrs and 10 Gyrs. The  $\delta$  absolute G magnitude and the  $\delta$  G-K magnitude using the empirical isochrones are found to be 0.35 and 0.1 respectively. Within these limits of Absolute G magnitude and G-K magnitudes, 11 objects are found to be parallel to the isochrones evolutionary track. To be able to classify these systems as binary, it is important to calculate the binding energy( $U_g$ ). If  $|U_g| > 2.5 \times 10^{33} J$ , the object will be considered as a binary system. The mass and the separation of the binary systems are estimated using the ATMO(BAHC15) model, which are then used for the calculation of absolute binding energy. 5 out of 11 objects are found to satisfy the binding energy condition and are considered to be the binary systems.

During this project, some sources that satisfy the matching algorithm are found not to be parallel to the theoretical or empirical isochrones. These objects are classified as strange systems. From the 142 prospective binaries, 12 systems are identified as strange systems. Upon investigation 2 of them are found to be known binary system which include Luhman16 AB and TWA 30AB. The investigation for the rest 10 objects requires the understanding of the known strange binary systems, which is the future step of this project.

### Acknowledgements

This work has made use of data from the European Space Agency (ESA) mission *Gaia* (<https://www.cosmos.esa.int/gaia>), processed by the *Gaia* Data Processing and Analysis Consortium (DPAC, <https://www.cosmos.esa.int/web/gaia/dpac/consortium>). Funding for the DPAC has been provided by national institutions, in particular the institutions participating in the *Gaia* Multilateral Agreement.

# Contents

<b>1</b>	<b>Introduction</b>	<b>5</b>
1.1	Binary System . . . . .	5
1.2	Gaia EDR3 . . . . .	5
1.2.1	Astrometric properties[2] . . . . .	6
1.2.2	Photometric properties[3] . . . . .	6
<b>2</b>	<b>Data processing</b>	<b>7</b>
2.1	Selection of Binary Systems . . . . .	7
2.1.1	Data query for Gaia objects . . . . .	8
2.2	Possible new binary systems . . . . .	9
2.3	Age of binary systems . . . . .	11
2.3.1	Model Selection . . . . .	11
2.3.2	Isochronic Systems . . . . .	12
2.3.3	Benchmark Binary systems . . . . .	12
2.3.4	Isochrones from unknown binary list . . . . .	14
2.4	Investigation of binary system . . . . .	14
2.4.1	Estimating mass . . . . .	14
2.5	Investigation for Strange Objects . . . . .	16
2.5.1	J0112-7031 . . . . .	16
2.5.2	J0138+8110A . . . . .	17
2.5.3	J0338-00061 . . . . .	17
2.5.4	J0419+2826 . . . . .	17
2.5.5	J1049-5319 . . . . .	18
2.5.6	J1132-3019 . . . . .	18
2.5.7	J1141+3813 . . . . .	18
2.5.8	J1231+4050C . . . . .	18
2.5.9	J1521+4336 . . . . .	18
2.5.10	J1536+3455A . . . . .	18
2.5.11	J1628-2428 . . . . .	19
2.5.12	J1839+4424B . . . . .	19
<b>3</b>	<b>Evaluation</b>	<b>20</b>
3.1	Known and Unknown Binary Systems . . . . .	20
3.2	Idp fraction values of binary system . . . . .	20
3.3	New binary systems . . . . .	21
3.4	Strange Objects . . . . .	22
<b>4</b>	<b>Conclusion and Future plans</b>	<b>24</b>
4.1	Conclusion . . . . .	24
4.2	Future Plans . . . . .	24
<b>A</b>	<b>Preview of Master_withDR3.csv</b>	<b>26</b>
<b>B</b>	<b>List of known binary systems used for cross-matching</b>	<b>30</b>
<b>C</b>	<b>Python Code</b>	<b>31</b>
	<b>Bibliography</b>	<b>34</b>

# List of Figures

2.1	H-R diagram with all objects and the primary and the secondary objects detected using criteria mentioned earlier in this section. The gray dots represent all objects that are part of this investigation. The black dots represent the primary object in the binary or multiple system. The blue plus symbol represent the secondary in the binary system. The primaries are mainly located in the upper section of the main sequence or in the white dwarf section while the secondary are located in the lower section of the main sequence. This validate the fact that primaries are heavier than secondaries. Hence, they evolve faster in comparison to the secondaries. . . . .	9
2.2	This figure shows all systems connected with their companions who found to be the possible candidate for new binary system. Gray dots represent all systems used for investigation. Blue plus symbols represent binary systems with lines connecting primary to their secondary. The system at $G = 20.0$ and $G-RP = 2.5$ system lies in the region of M/T dwarf. . . . .	10
2.3	ATMO(BAHC15) data is used to plot the ages and the masses over the data.(Left) The isochrones between 0.5Mys to 10Gyrs. (right) Masses on the data between $0.01M_{\odot}$ and $0.5M_{\odot}$ which is the upper limit of the mass in the data. . . . .	12
2.4	All known binaries found by our algorithm is shown with the isochrones from ATMO(BAHC15) on Absolute G magnitude vs G-K colour magnitude diagram. The lines joins the pair of binaries denoted by triangles. The coloured lines represent the isochrones of age $\leq 1.0$ Gyrs . . . . .	13
2.5	Binary candidates with isochronic fitting from ATMOS(BACH15). Black line represent the ages and blue line represent the mass of the objects in solar masses $M_{\odot}$	14
2.6	The plot shows the binary systems connected together in black solid line. The broken black line represent the age of the isochrones with ages less than 0.1Gyrs. The same mass objects are represented by the broken blue line. The primary and its companion are represented in the triangles. The number on the primary component of the system an be used to find the 'SHORTNAME' of the object and its secondary in the legend at the bottom of the H-R Diagram. . . . .	15
2.7	Binary systems that do not show typical behaviour and hence are interesting to study as part of this investigation. The objects are either too far, or have very similar absolute magnitude or at different stage of star life than expected. . . . .	17
3.1	Above histogram shows the number of the primary objects of the (left) known binary systems and (Right)possible(prospective)binary systems with different <code>idp_frac_multi_peak</code> . This shows the distribution of the values of the idp fraction as percentage. In both cases the known binary systems and the binaries that are possible candidates for the binary systems, the numbers of the objects with idp fraction value greater than 50 is very small. . . . .	21
3.2	Binary candidates with isochronic fitting from ATMOS(BACH15). Black line represent the ages and blue line represent the mass of the objects in solar masses $M_{\odot}$	23

# List of Tables

2.1	Primary and secondary object with their basic properties. These objects shows strange behaviour but satisfied with the binary criteria used in our investigation. Parallax is measured in mas, separation in AU and Binding energy in joules. . . .	11
2.2	Isochronic model and their properties . . . . .	11
2.3	Primary and secondary object with their basic properties.the separation is given in au and parallax is in arcsec.In bold Star_A J0433+1810 is the primary with 2 companions J0433+1758 and J0433+1750 which makes it a triple system. . . . .	15
2.4	Estimate of the masses of the star A and the star B from the masses of the isochrones. Bold Star_A J0433+1810 with one of the companions J0433+1758 have N/A as its mass. The estimated mass is not available as this does not have G-K magnitude. .	16
3.1	The objects that are considered for the final list of the object as this satisfy all the conditions. As J0433+1810 could be the triple system. Hence this is not considered for the further investigation at this point. Hence, 10 out of 11 is considered for the investigation. Base on the estimated mass the absolute energy of the binding energy of the systems is calculated. . . . .	21
3.2	This is the final list of the binaries that satisfy all conditions. The objects satisfy the initial conditions of separation. proper motion and parallax difference. These are also found to be isochrones and also have absolute binding energy greater then the minimum energy required [4] . . . . .	22
3.3	Primary and secondary object with possible classification and spectral values. . . .	22

# Chapter 1

## Introduction

Binary stars references can be found in scriptures that are as old as Aryan civilisation, where most of the objects in the sky are described as a person in these stories. The first reference of binary star is found in the form of two yogic married couple Arundhati and Vasistha known as Alcor and Mizar respectively, while the first scientific reference is found in 1802 by Sir William Herschel, who observed binary systems and catalogued them.

### 1.1 Binary System

Binary systems are defined as the system of two stars that revolve about common centre of mass and they are gravitationally bound to each other. These are formed at similar time and gravitationally bound to each other due to the separation and the masses of the objects. This bond results in several properties that can help to detect binary system. These properties include the difference between proper motion, angular separation, parallax, position angle and binding energy. Due to the complex nature of the binary systems, it is not possible to provide a clear boundary for these properties.

Binary systems are classified into close and wide binaries based on the separation, although no clear separation boundary is defined to differentiate between close and wide binaries.

Binaries are divided into following categories:

- Visual binaries: Two stars can be viewed through telescope as they have wide enough separation.
- Spectroscopic binaries: Binaries are quite close and not possible to resolve through visual observation. The Doppler-shift in their spectra can be used to detect these type of binaries. Blue-shifted, red-shifted and Tangential motion with a period can be used to identify the pair.
- Eclipsing binaries: These binaries are detected using the photometric measurements. The detection of the change in their apparent magnitude with specific period provides us the evidence of these systems being binary.
- Astrometric binaries: Astrometric binaries are detected using the wobbling in proper motion due to the gravitational effect from its companion. This is periodic in nature which is due to the fact that they move about the same centre of mass.

### 1.2 Gaia EDR3

The Gaia EDR3 contains the data from 25th July 2015 to 28th may 2017[5]. This dataset provides us more information in comparison to the DR2. The EDR3 contain approx. 130,000 more objects in comparison to DR2 making total of approximately 1.8 billion objects. Several new parameters has been introduced in EDR3, and the full description can be found on Gaia EDR3 documentation<sup>1</sup>.

---

<sup>1</sup>[https://gea.esac.esa.int/archive/documentation/GEDR3/Gaia\\_archive/chap\\_datamodel/sec\\_dm\\_main\\_tables/ssc\\_dm\\_gaia\\_source.html](https://gea.esac.esa.int/archive/documentation/GEDR3/Gaia_archive/chap_datamodel/sec_dm_main_tables/ssc_dm_gaia_source.html)

In this project, the coordinates ‘RA’ and ‘DEC’ are J2000, while the coordinates in the EDR3 are J2016.

The Luminosity function[6] of the primaries is used in order to differentiate between the single stars and the binary sources. In the simulated model, the properties of the secondary objects are obtained using Hess diagram distribution. The CCDs produced raw data which is used to process in order to get useful information. The information like astrometric, photometric properties are obtained using the data produced by Initial Data Treatment system. In order to get the sky mapper and astrofield detailed, several models were calibrated. [7].

### 1.2.1 Astrometric properties[2]

The columns defined in the Gaia EDR3 that are useful for this project are G, G\_rp, idp\_frac\_multi\_peak, proper motion in RA and DEC, and parallax. The EDR3 contains complete list of the objects with G within the range of 11 to 17. The bright objects are not well defined in EDR3.

The uncertainty is 0.01-0.02 mas when G is less than 15 mag, 0.05 mas when G equals to 17 mag. It increases to 0.4 mas when G is 20 mag and further increases to 1.0 mas when G is 21 mag.

Similar pattern has been observed for parallaxes. For G less than 15mag, the uncertainty is around 0.02mas to 0.03 mas, and when G is 17 mag, the uncertainty is 0.07 mas, while for G equals to 20mag, it increases to 0.5 mas. It further increases to 1.3 mas when G is 21 mag [2].

The uncertainty increases rapidly when G is between 17mag and 21 mag. The increases in the uncertainty is highest when G changes from 20 mag to 21 mag.

### 1.2.2 Photometric properties[3]

The errors in the photometric measurements show the similar behaviour as the astronomical properties. The uncertainty is small when G is up to 13 mag, and it increases rapidly till G equals to 20 mag.

The uncertainty in the G band is found to be approximately 0.3 mmag for G smaller than 13 mag. It increases to 1 mmag when G reaches 17mag, and further increases to 6 mmag when G is 20 mag[3].

The uncertainty in the G\_BP band is found to be about 0.9 mmag for G less than 13 mag, and it increases to 12 mmag when G is 17mag, and further increase to 108 mmag when G reaches 20 mag [3].

The uncertainty in the G\_RP band is found to be around 0.6 mmag for G under 13 mag, and the uncertainty increases to 6 mmag when G is 17mag, and further increases to 52 mmag when G reaches 20 mag [3].

The errors in the photometry are the lowest in the G band magnitude, while it is highest in the G\_BP band. The uncertainties in the G\_BP and G\_RP bands for G = 20mag are quite high. This difference could cause a high level of uncertainty when using G-G\_RP or G-G\_BP as colour magnitudes. The objects with G magnitude greater than 17 shows some unexpected nature due to the uncertainty in the magnitude.

No new astrophysical parameters are defined in the EDR3. All astrophysical parameters are same as DR2 data release. Further information on GAIA DR3 can be found on Gaia EDR3 website<sup>2</sup>.

---

<sup>2</sup><https://gea.esac.esa.int/archive/documentation/GEDR3/index.html>



## Chapter 2

# Data processing

### 2.1 Selection of Binary Systems

The data used for analysis here is provided by Prof.R.Smart. The data contains 14280 objects. Most of them are from Gaia EDR3 and some of them are from 2MASS or WISE surveys. The binary systems are detected by cross matching the list by itself<sup>1</sup>. To ensure the detection of the binary systems, the following conditions are used to detect the binary system within the dataset[8]:

- $\rho < 100 \times \omega$  (*in mas*)
- $\Delta\omega < \max[3\sigma_\omega, 1.0\text{mas}]$
- $\Delta\mu < 0.1\mu$
- $\Delta\theta < 15^\circ$

where  $\rho$  represents the separation between the primary and the secondary objects in arc-seconds, and  $\Delta\omega$  is the difference between the parallaxes of the primary and the secondary objects.  $\Delta\omega$  need be to smaller than  $3\sigma_\omega$  mas or 1.0 mas, whichever is greater, where  $\sigma_\omega$  is the parallax of the primary object in the system. This allows to detect the system with significant proper motion. Besides, the separation between the objects is enough to maintain the minimum amount of the binding Energy required to be in the bound system. Some objects may have unrealistically low error and hence the 1.0 mas is necessary to accommodate these small parallax errors[1]. The detection of the false positives is a problem when choosing these conditions. Relaxing the conditions may result in a increased number of false positives, while strict conditions may result in losing binary systems. Hence, these conditions are chosen with significant considerations.

To reduce the false positive detection while not losing the potential systems, the third (proper motion) and the fourth (position angle) conditions are used. The difference of the proper motion ( $\Delta\mu$ ) between the primary and secondary must be less than the 10% of the proper motion of the primary object. The proper motion of a object is calculated using equation 2.1

$$\mu = \sqrt{\mu_{ra}^2 + \mu_{dec}^2} \quad (2.1)$$

The proper motion in the RA and DEC is provided in the data under columns **PMRA** and **PMDEC** respectively. The proper motion difference should be less than the 10% of the proper motion of the brightest object within the system. For some co-moving system, the proper motion of the objects may be significantly small but they may not be gravitationally bound to each other. Therefore the position angle will help to filter out the systems that are not gravitationally bound.

$$\theta = \arctan\left(\frac{\mu_{Ra}}{\mu_{dec}}\right) \quad (2.2)$$

The position angle in degrees of the object is calculated using equation 2.2. The difference in the position angle between the primary and the secondary must be less than  $15^\circ$ . The will help

---

<sup>1</sup>The code used in this project can be found on github <https://github.com/as-uh/MSc-data-Science-project/tree/main/code>

to select the objects that have relative orbital motion about a common centre. This could be true for multiple systems and may result in the detection of triple or quadruple systems.

Not all objects in this dataset contain value for parallax, where the missing value is recorded as  $-99999$ . As these objects do not have parallax, it is not possible to check certain conditions for binarity. Only the objects with parallax  $> 0$  are included in this investigation. Out of 14280 objects 3577 objects have negative parallax and 10702 objects with parallax in dataset. This is still a considerable amount of the objects as only 25.05% of the data is not part of our investigation, which leaves us with 74.95% of the data available for investigation.

These criterion provide us a significant amount of the system that are potential candidates for the binary systems. 480 out of 10702 objects are detected as a part of binary, triple, quadruple or multiple system. Although the criterion are very strict, there is still a significant chance of detecting false positives. When detecting the companion of each object in the dataset, the cross-matching inside the dataset may have created multiple entries while detecting multiple star systems. In order to detect and combine these systems, the systems with common component are considered as part of one system.

In general, the brightest object is considered to be the primary in the system. However, when detecting binary systems, the brightness is not taken into consideration. **GAIA**<sub>G</sub>, which is the G-magnitude of an object is used to calculate the absolute G magnitude. This allows to allocate the systems into primary and secondary categories. The brightest object in the system will be labelled as primary and rest will be secondary. The system in which the **GAIA**<sub>G</sub> value for one of the object is not available, the object with G-magnitude value is considered as primary and other as secondary.

This can be seen in the H-R diagram 2.1 that most of the primary objects are at the brighter end of the HR diagram in comparison to the secondary objects. There are some binary systems bound to white dwarfs with their secondary object lie on the main sequence. The objects in this H-R diagram are available in GAIA EDR3 if not then DR2 values are used. The objects that are not present in the Gaia could not be considered as no Absolute G magnitude and G-RP value could not be retrieved. This was achieved using **GAIA**<sub>TOG</sub>  $> 0$ , where **GAIA**<sub>TOG</sub> represent the positive detection of a system by Gaia. This will in result provide us a list of the systems with 228 systems which include both known and possible new systems.

### 2.1.1 Data query for Gaia objects

The data present in the dataset provide us general information about the objects from the GAIA EDR3, while there are other properties such as **idp\_frac\_multi\_peak** could be useful for the selection of binary systems. In addition to the new information from the EDR3, it will also validate the information in the dataset used. As some of the information used in our dataset comes from the GAIA DR2 or other surveys like SDSS (Sloan digital Sky Survey) and 2MASS (Two-Micron All Sky Survey). This project focuses on the data from Gaia, it is important to have the values such as parallax, proper motion and Gaia colours updated according to EDR3 which provide more accurate data in comparison to previous data releases.

This is done using the topcat astronomical software<sup>2</sup>. Which runs query using stilt, based on the java. The stilt query could be run in the Jython, which allows the use of python syntax in java. The fact that it runs on java makes it difficult integrate it in the python script and could be time consuming. The topcat UI is time efficient method to retrieve the data from the Gaia public library. Topcat provide us a query feature 'cone' provided with the library with astronomical database from different surveys.

The coordinated of the objects in the dataset used may be slightly different from the coordinated of the objects in the Gaia EDR3. The exact match is also not possible due to the different significant number of digits in the Gaia EDR3 data and our dataset. The search is run on the ra and dec in degrees within the radius of 5 arcsec. This will allow us to cover the possible error in the ra and dec due to the change in location caused by the motion of the object in the sky.

The results of this query is run using the cone url<sup>3</sup> for Gaia EDR3 database at ESA. The data from the cone search and the our dataset is combined together in order to compare the values, the value of the different colour magnitudes from the other surveys and the spectrometry

<sup>2</sup><http://www.star.bris.ac.uk/~mbt/topcat/>

<sup>3</sup>[https://gea.esac.esa.int/tap-server/conesearch?TABLE=gaiaedr3.gaia\\_source&IDCOL=source\\_id&RACOL=ra&DECCOL=dec](https://gea.esac.esa.int/tap-server/conesearch?TABLE=gaiaedr3.gaia_source&IDCOL=source_id&RACOL=ra&DECCOL=dec)

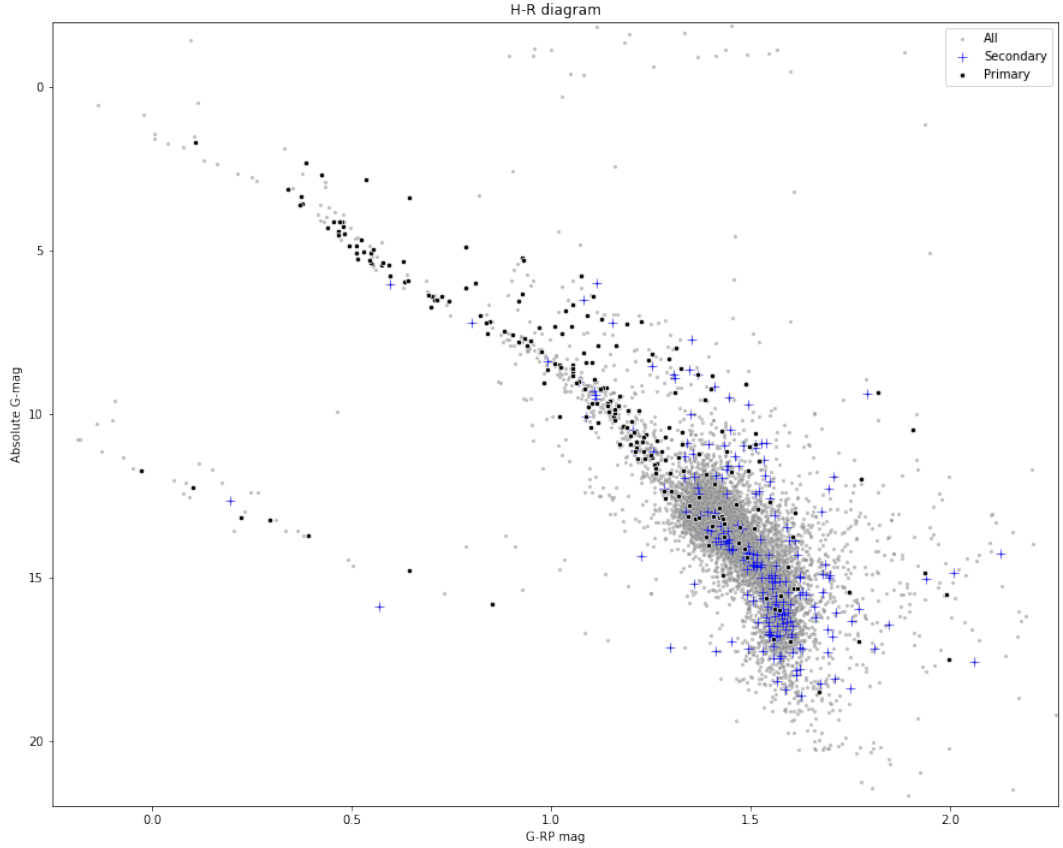


Figure 2.1: H-R diagram with all objects and the primary and the secondary objects detected using criteria mentioned earlier in this section. The gray dots represent all objects that are part of this investigation. The black dots represent the primary object in the binary or multiple system. The blue plus symbol represent the secondary in the binary system. The primaries are mainly located in the upper section of the main sequence or in the white dwarf section while the secondaries are located in the lower section of the main sequence. This validates the fact that primaries are heavier than secondaries. Hence, they evolve faster in comparison to the secondaries.

information. The number of the objects that matched with the objects in the GAIA EDR3 cone search 11369 out of 14279 from the our dataset. This makes the 76% of the data from the dataset available in the Gaia EDR3. This may increase with the release of full DR3 and hence will be able to expand out research.

## 2.2 Possible new binary systems

From 228 systems some of the systems are known systems. These systems can be filtered out by cross matching with the list of known binary objects from [9] and others. This will allow to focus on the objects that may possibly be new binary systems. The list of known binary systems contains 107173 binary systems. If either secondary or the primary of our detected system is in this list then it is considered as a known system. After careful consideration of the possible error in RA and DEC positions due to the epoch. Out of 228, 86 objects are found to be the known systems. Using this method two lists are formed one which contains the known binary systems containing 86 systems and other with probable new systems (Unknown systems) with 142 systems.

Although the known binary system list contains all of the possible objects but it is not possible

to record every system. This is due to the lack of proper catalogue for binary systems. As several research take place since the list was made and hence need to investigate the objects in the list of unknown binaries carefully.

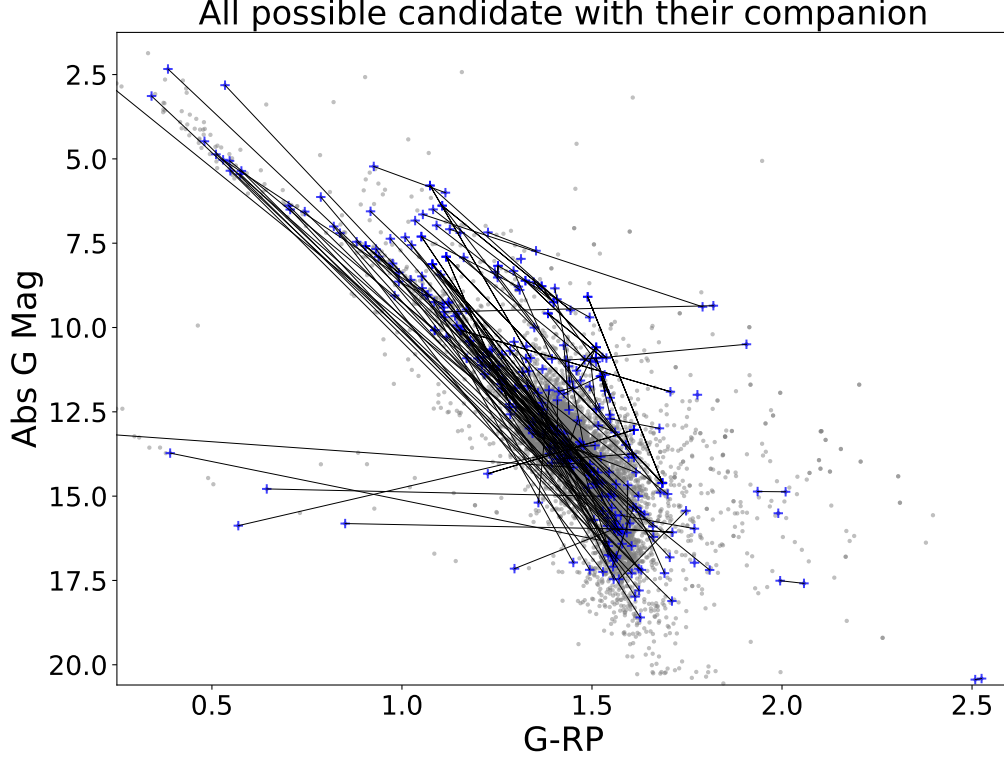


Figure 2.2: This figure shows all systems connected with their companions who found to be the possible candidate for new binary system. Gray dots represent all systems used for investigation. Blue plus symbols represent binary systems with lines connecting primary to their secondary. The system at  $G = 20.0$  and  $G-RP = 2.5$  system lies in the region of M/T dwarf.

It is clear from the H-R diagram in figure 2.2 that some of the objects that matches criteria to be binary systems are showing some strange behaviour. Considering that binaries are isochrones, we have selected few systems that do not follow that typical behaviour and require further investigation. The objects that are found to have strange behaviour using visual analysis are in table 2.1. Out of 157 these 12 systems require further investigation in order to explain their strange nature. The reasons these are considered as strange is either they are very far or both primary or secondary seems to have similar brightness in Absolute G magnitude and do not have same ages.

The binding energy calculated in the table 2.1 are calculated with assumption that mass of every object is  $0.5M_{\odot}$ , which is approximately upper limit of the mass of the objects in the data used. The formula used for the calculation of the binding energy is

$$|U_g| = -\frac{GM_1M_2}{d} \quad (2.3)$$

where,  $|U_g|$  represent the absolute value of the binding energy,  $M_1$  and  $M_2$  are the mass(in kg) of the Primary and the secondary object and  $d$  is the separation(in m) between the primary and the secondary objects. From above equation,  $|U_g| \propto M_1M_2$ , as the mass decrease the absolute binding energy decrease. The classical empirical limit for a system to considered as physically bound is  $|U_g| > 10^{33} J$  [4][10].  $|U_g| \propto \frac{1}{d}$ , increase in the separation will result in the smaller values. In this investigation the separation is calculated using RA and DEC values in AU provided in table 2.1.

Star_A	p(arcsec)	AbsG	G-RP	Star_B	d(AU)	$ U_g $ (J)
<i>J0112 – 7031</i>	20.791	14.863	1.936	<i>J0112 – 7031A</i>	2319.746	$1.901e + 35$
<i>J0138 + 8110A</i>	24.321	15.327	1.609	<i>J0138 + 8110B</i>	21844.149	$2.019e + 34$
<i>J0338 – 00061</i>	7.250	13.750	1.605	<i>J0338-0006</i>	358313.719	$1.231e+33$
<i>J0419 + 2826</i>	7.734	6.647	1.055	<i>J0419+2827</i>	57989.658	$7.605e+33$
<i>J1049 – 5319</i>	496	20.409	2.525	<i>J1049-5319B</i>	0.184	$2.391e+39$
<i>J1132 – 3019</i>	21.089	11.859	1.387	<i>J1132-3018</i>	15329.978	$2.877e+34$
<i>J1141 + 3813</i>	8.119	12.758	1.462	<i>J1141+3820</i>	630659.428	$6.992e+32$
<i>J1231 + 4050C</i>	16.485	9.353	1.819	<i>J1231+4050B</i>	9515.380	$4.634e+34$
<i>J1521 + 4336</i>	10.307	13.496	1.508	<i>J1521+4336A</i>	62143.459	$7.096e+33$
<i>J1536 + 3455A</i>	15.856	12.156	1.409	<i>J1536+3455</i>	16533.303	$2.667e+34$
<i>J1628 – 2428</i>	7.238	11.451	1.522	<i>J1628-24281</i>	123337.242	$3.575e+33$
<i>J1839 + 4424B</i>	26.545	15.434	1.748	<i>J1839+4424A</i>	16141.268	$2.732e+34$

Table 2.1: Primary and secondary object with their basic properties. These objects shows strange behaviour but satisfied with the binary criteria used in our investigation. Parallax is measured in mas, separation in AU and Binding energy in joules.

## 2.3 Age of binary systems

The age of the primary and secondary is also a very important part of the test for binary system. The isochronic model fitting is used to investigate the age of the systems. This will also allow to investigate the characteristics of the system based on the composition.

### 2.3.1 Model Selection

The selection of model is very important part of this investigation. The correct model will help to identify the age and mass of the system. Several Isochronic models were investigated including MIST, YaPSi, Parsec, SPOTS and ATMO (BAHC15) model. The range of masses included and the properties on the objects in these models are different as shown in table 2.2. Most of the models do not cover the range of the masses that are required in our investigation.

Model Name	Lower limit	Upper limit	Comment
MIST [11]	$0.1M_{\odot}$	$350M_{\odot}$	Focused on Massive star
YaPSi [12]	$0.15M_{\odot}$	$5.0M_{\odot}$	Focused on $M \leq 0.6M_{\odot}$
PARSEC [13]	$0.1M_{\odot}$	$350M_{\odot}$	Relevant $M > 0.5M_{\odot}$
BaSTI [14]	$0.1M_{\odot}$	$15.0M_{\odot}$	out of required range
SPOTS [15]	$0.1M_{\odot}$	$1.3M_{\odot}$	Out of required range
ATMO(BAHC15) [16]	$0.1M_{\odot}$	$1.5M_{\odot}$	Focused low mass Stars

Table 2.2: Isochronic model and their properties

The range of the masses of binary candidates in this analysis have range of  $0.01M_{\odot} \sim 0.5M_{\odot}$ . This range of mass is included in the ATMO grid model BAHC15 [17]. This model focused on low-mass stars with age ranges from 0.005 Gys to 10 Gys. While for the other models mentioned in the table 2.2 the mass of the stars do not satisfy the range of the masses and also focused on the evolutionary models of the massive stars. While the models like YaPSI [12] focuses on the masses lower than  $0.6M_{\odot}$  but the lower limit for this is  $0.1M_{\odot}$ , hence do not satisfy the required mass range.

Due to the mass range of include in the ATMO(BAHC15) isochrone is the key factor to choose this data. Figure 3.2 indicate that most of the objects included in the data used in this investigation had mass  $< 0.5M_{\odot}$ . This mass range is only covered in the ATMO(BAHC15) model. This data also provide the Gaia colour magnitudes along with other properties including luminosity ratio, effective temperature, radius and other features. Gaia colour magnitudes will help us to superimpose isochrones on our data in order to estimate the mass and age of the objects. Hence, it will allow us to calculate the closest estimated value of the Binding energy of the systems.

There are several models described in ATMO(BAHC15) [16], which used similar evolution model algorithm. The BACH15.GAIA<sup>4</sup> contain the data with Gaia magnitudes which include G, R, BP magnitudes that can be use to compare the data on colour magnitude H-R diagram. This will allow to estimate the age and mass of different systems.

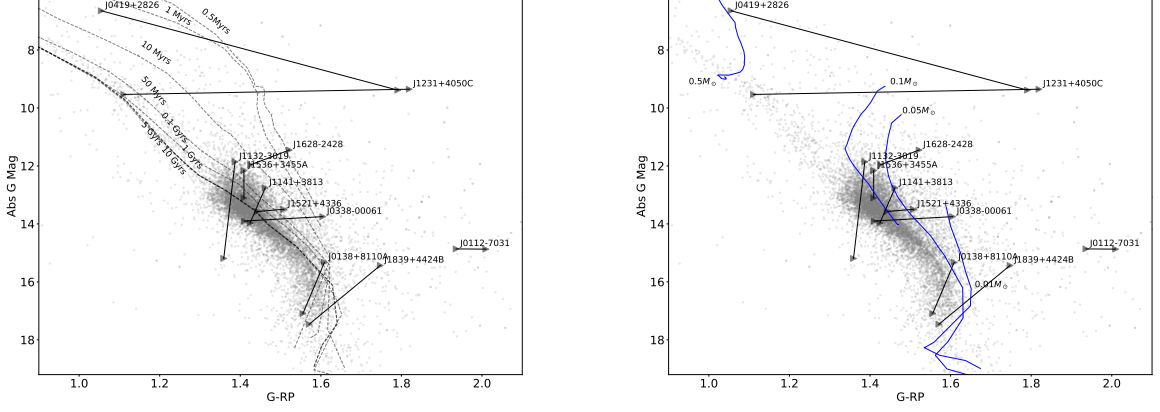


Figure 2.3: ATMO(BAHC15) data is used to plot the ages and the masses over the data. (Left) The isochrones between 0.5 Myrs to 10 Gyrs. (right) Masses on the data between  $0.01M_{\odot}$  and  $0.5M_{\odot}$  which is the upper limit of the mass in the data.

The figure 2.3 shows that the upper limit of the masses in the data used for this investigation is  $0.5M_{\odot}$  which was the assumed mass for the calculation of the binary system. As the actual mass of the objects are smaller than the assumed mass for the calculation of the binding energy. Hence, the actual value of the binding energy will be smaller than the binding energy of the system.

The model is not well optimised for the smaller masses ( $m < 0.7M_{\odot}$ ) [16]

### 2.3.2 Isochronic Systems

The binary systems are formed together in the universe and hence the age of the binary systems must be isochrones (Must have same age). The age of the systems can be estimated using the theoretical isochrones in ATMO(BAHC15) [16]. Due to the complex nature of the stars it is not possible to simulate the exact conditions as in the real stars and hence the isochrones cannot provide us the exact values. The values hence calculated are acceptable due to the small percentage error.

From figure 2.3 and figure 3.2 it is clear that the theoretical isochrone lines with  $age \geq 0.1 Gyrs$  overlapping with each other and hence will be difficult to estimate the age of the systems that are close to these lines. The difference between the ages is quite large and hence it will not be ideal to consider these isochrone lines to estimate the age of the system. The theoretical isochrones with values greater than 0.8 Gyrs is are considered to identify the isochronic systems in list of the object that qualify the initial criteria for the separation, proper motion, parallax and the position angle. As not all ages are available and it will not be possible to get the exact age of the systems due to the reasons mentioned earlier hence the calculations are made within the acceptable suitable error. The unresolved binaries are difficult to fit on the theoretical isochrones. This also cause the uncertainty in the models as binaries can't be fit in the single star models [18].

### 2.3.3 Benchmark Binary systems

To be able to understand and explain the nature of the objects in list of unknown binary system list of known binary is used. The list of known binaries can be used to define the behaviour. It is important to understand the relation between the known binary system data and the theoretical isochrones. This can be used as benchmark to refine the systems that shows the isochronic nature. This will reduce the data loss and improve the accuracy of the results produced.

<sup>4</sup>[http://perso.ens-lyon.fr/isabelle.baraffe/BHAC15dir/BHAC15\\_iso.GAIA](http://perso.ens-lyon.fr/isabelle.baraffe/BHAC15dir/BHAC15_iso.GAIA)

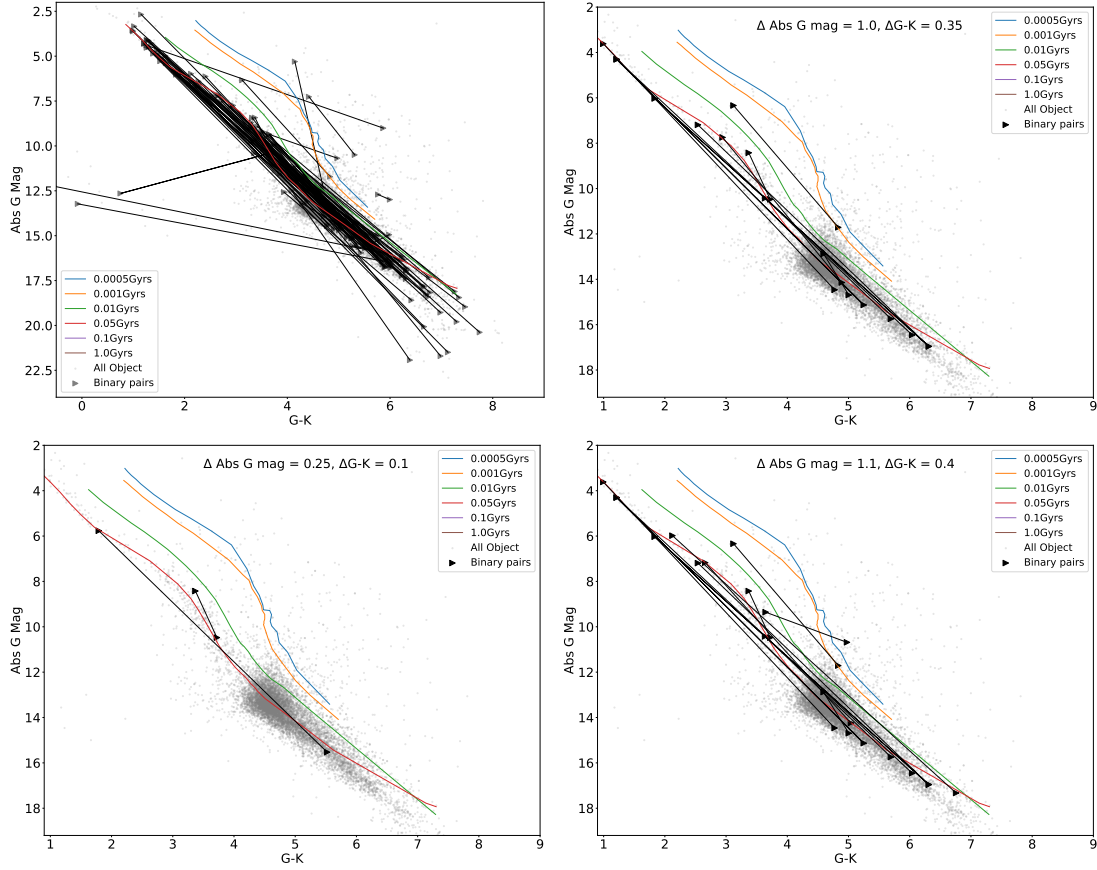


Figure 2.4: All known binaries found by our algorithm is shown with the isochrones from ATMO(BAHC15) on Absolute G magnitude vs G-K colour magnitude diagram. The lines joins the pair of binaries denoted by triangles. The coloured lines represent the isochrones of age  $\leq 1.0$  Gyrs

The binaries are spread over a large range and some of them have strange nature as shown in figure 2.4(left). While most of the binaries are showing the expected nature i.e the isochronic nature. Some of the binaries are showing unexpected behaviour. The binarity and the nature of the objects with the strange nature in the unknown binary list can be explained using these binaries with strange nature. Although it is important to investigate these objects to understand the credibility by checking alignment of the data with the GAIA data. There are also some binaries with one of the companion as white dwarf. These binaries cannot be detected on the theoretical isochrones as these do not include the evolution of the white dwarfs. The white dwarfs can be used to determine the age of the binaries. It could be useful to find the empirical isochrones while that is beyond the scope of this project. Hence, the binary system with one of their companion as white dwarfs are being excluded.

The theoretical are not exactly aligned with the lines joining the primary and secondary companions. As the isochrones do not contain the data that can be used to draw isochrones with mass at regular interval and ages. Also it is not easy to describe the exact nature of the stars evolution using isochrones. The nature and the evolution is very complex process and hence isochrones are only close approximation of it. This will cover the binaries within the possible error of the theoretical isochrones. In order to determine the suitable upper and lower limits of the absolute G magnitude and the G-K colour magnitude trial and error method is used. We stated with the small value and increase its value in order to achieve best results. The value initial values of  $\Delta \text{Abs G mag}$  and  $\Delta \text{G-K}$  is considered as 10 percent of the interval in the plot. The starting value for the  $\Delta \text{Abs G mag}$  is 0.25 and for  $\Delta \text{G-K}$  is 0.1. Here it is important to consider the fact that the age of the isochrones considered less than 0.1 Gyrs and hence the proportion of the binary systems detected will not be close to 100% as it contains binary that have age  $\geq 0.1$  Gyrs. Hence it is also important to consider plot shown in figure the graph of the binary systems selected during the process in order to include any system that may have age outside our set boundaries. After several

tries the values of  $\Delta \text{Abs G mag}$  is 1.0 and for  $\Delta \text{G-K}$  is 0.35. Using these values 8 out of 86 was found to be the binaries within the boundaries. Which is 9.3%, it seems a very small proportion of the total binaries in the list. But this is due to the exclusion of the binaries with white dwarfs as a companion, binaries with strange behaviour and also the binaries with age  $\geq 0.1 \text{ Gyrs}$ . Increasing the limit in order to get more binary systems included will result in the binary systems that do not show typical behaviour or have age  $\geq 0.1 \text{ Gyrs}$  as shown in the figure 2.4(bottom right).

The another limitation of this model is that if the binary system is very young (age  $< 0.4 \text{ Myrs}$ ) it will not detect those systems. This is due to the values of the  $\Delta \text{Abs G mag}$  and  $\Delta \text{G-K}$  chosen in such a way that there will be less overlap between the two ages included in the ATMO(BAHC15) isochrones.

The figure 2.4(right) shows the binaries systems that are being detected using these limits for the absolute G magnitude and the G-K magnitude. The comparison between figure 2.4 left and right shows that that the binaries only the binaries that are parallel to the isochrones are selected.

### 2.3.4 Isochrones from unknown binary list

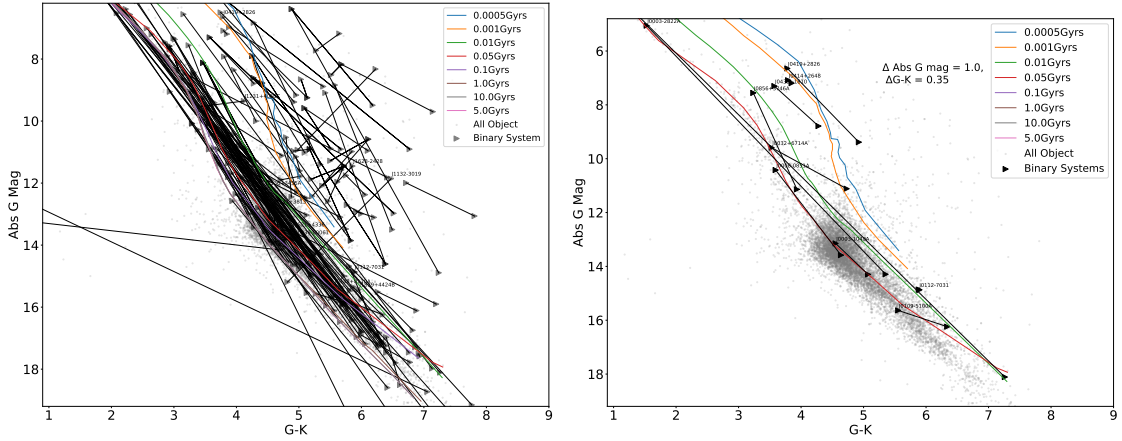


Figure 2.5: Binary candidates with isochronic fitting from ATMO(BACH15). Black line represent the ages and blue line represent the mass of the objects in solar masses  $M_{\odot}$

These limits now can be applied to select the binaries that are satisfy the conditions of being isochrones. Out of 157 systems only 11 objects are found to be binary systems that satisfy these conditions. Which is 7.1% of the total number of objects. Which is consistent with the data from the benchmark. This shows that less than 10% of the binary system have age  $\leq 0.1 \text{ Gyrs}$ . The figure 2.5 shows the side by side comparison between the unknown binary systems and the filtered binary system with the boundaries of benchmark systems.

From table 2.3 the object J0433+1810 is found to be a binary system although when investigated closely it is a triple system with J0433+1758 and J0455+1750 as its companions. The nature of the triple system is complicated than the systems the simple binary systems. Due to this complicated nature the binding energy boundary cannot be used to validate the results as the value of the binding energy limiting value for triple system will be different than the binary system. The gravitational force between the objects will be different than the binary system in order for the system to be stable.

In order to calculate the values of the binding energy of the systems the mass of the systems can be interpolated using the mass of the isochrones. These masses can be use to calculate the close estimate of the absolute binding energy. And hence will be able to check if these binary systems satisfy the binding energy or not.

## 2.4 Investigation of binary system

### 2.4.1 Estimating mass

The estimation of mass is based on the mass of the theoretical isochrones ATMO(BACH15). The calculation of the mass is based on the time period of the binary systems. Sometimes it is not



Star_A	Parallax	AbsGmag	GAIA_GR	Star_B	separation
J0003-1040A	14.825	13.147	1.406	J0003-1040	40684.160
J0008-0851A	10.288	10.422	1.177	J0008-0851	3513.411
J0856+3746A	9.616	7.557	1.025	J0856+3746B	161748.918
J0109-5100A	62.789	15.636	1.539	J0109-5100	28333.978
J0112-7031	20.791	14.863	1.936	J0112-7031A	2319.746
J0032+6714A	101.086	9.590	1.146	J0032+6714B	1400.342
J1112+3548A	44.058	4.479	0.480	J1112+3548	20099.720
J0414+2648	7.890	7.086	1.126	J0414+2646	15517.111
J0003-2822A	24.831	5.059	0.547	J0003-2822	2721.436
J0419+2826	7.734	6.647	1.055	J0419+2827	57989.658
<b>J0433+1810</b>	6.942	7.303	1.051	<b>J0433+1758</b>	331409.403
				<b>J0433+1750</b>	23841.506

Table 2.3: Primary and secondary object with their basic properties. the separation is given in au and parallax is in arcsec. In bold Star\_A J0433+1810 is the primary with 2 companions J0433+1758 and J0433+1750 which makes it a triple system.

possible to measure the time period of the system. In case the spectrometry is use to estimate the mass. The calculation of the mass in this way is beyond this project. The mass of the binary systems is calculated based on the mass of the isochrones.

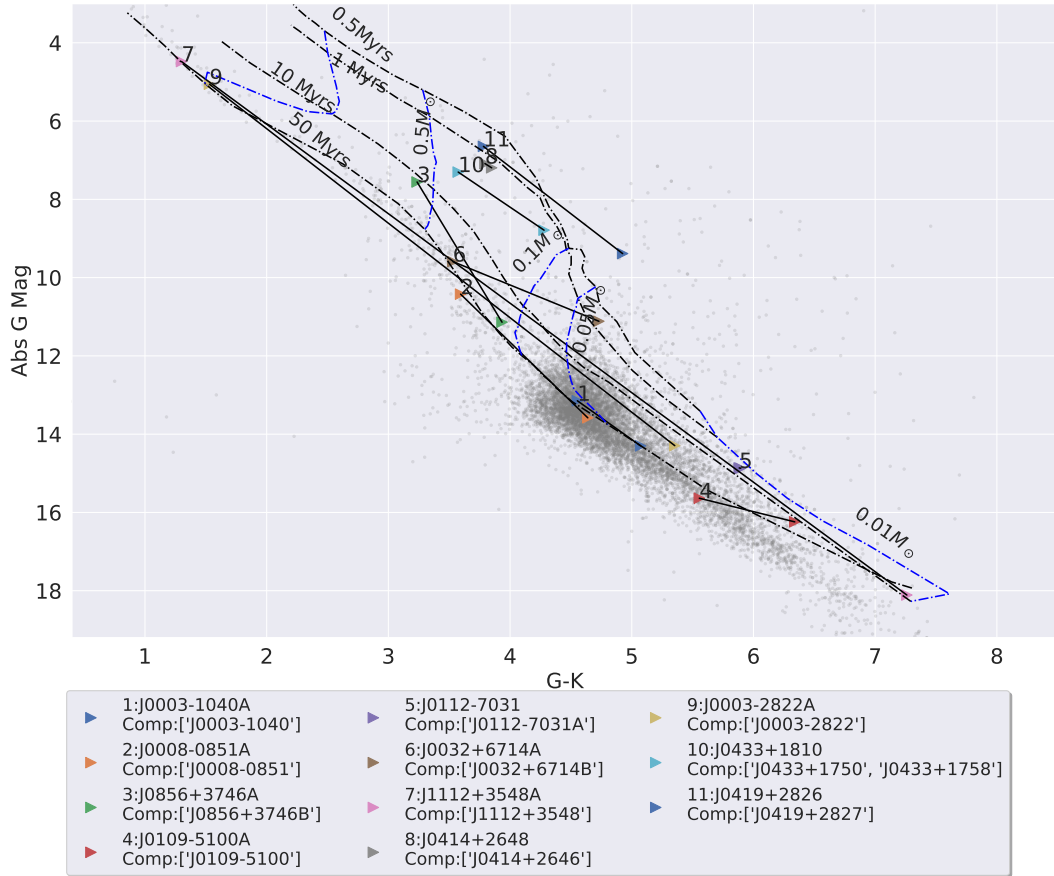


Figure 2.6: The plot shows the binary systems connected together in black solid line. The broken black line represent the age of the isochrones with ages less than 0.1Gyrs. The same mass objects are represented by the broken blue line. The primary and its companion are represented in the triangles. The number on the primary component of the system can be used to find the 'SHORTNAME' of the object and its secondary in the legend at the bottom of the H-R Diagram.

The comparison of the age and mass together of the unconfirmed binary systems are shown in the figure 2.6. The mass calculated in this way will be a close estimate of the real mass of the system. This will be useful to get the close estimation of the binding energy of the system.

Star_A	Mass_A( $M_{\odot}$ )	Star_B	Mass_B( $M_{\odot}$ )
J0003-1040A	0.055	J0003-1040	0.04
J0008-0851A	0.2	J0008-0851	0.055
J0856+3746A	0.6	J0856+3746B	0.13
J0109-5100A	0.35	J0109-5100	0.02
J0112-7031	0.15	J0112-7031A	0.15
J0032+6714A	0.3	J0032+6714B	0.03
J1112+3548A	1.1	J1112+3548	0.015
J0414+2648	0.35	J0414+2646	0.35
J0003-2822A	1.0	J0003-2822	0.2
J0419+2826	0.4	J0419+2827	0.06
<b>J0433+1810</b>	0.5	<b>J0433+1758</b>	N/A
		<b>J0433+1750</b>	0.15

Table 2.4: Estimate of the masses of the star A and the star B from the masses of the isochrones. Bold Star\_A J0433+1810 with one of the companions J0433+1758 have N/A as its mass. The estimated mass is not available as this does not have G-K magnitude.

The masses of the primary and the secondary objects are shown in the table 2.4. The masses are close estimate only. The J0433+1758 one the companion of J0433+1810 mass is not predicted in the table above. In figure 2.6 J0433+1810 only have one object connected to one object. This is due to the fact that J0433+1758 does not have similar age as the primary and hence it is not selected as a part of the system. This object is triple star system. Before making any conclusions about this system being a co-moving stars or the binary system. It is important to do further observations.

During this investigation the object with greatest absolute G magnitude is considered as star A(primary) and rest of them are considered as Star B (Secondary). Considering the fact that both of the stars have same age, the star with higher mass will brighter and the lower mass will be dimmer. Upon observing the values of the masses in table 2.4 the masses of the Star A is greater than the mass of the Star B. This validates the values of the masses and the absolute G magnitude follows the general trend.

## 2.5 Investigation for Strange Objects

In order to understand the behaviour it is important to investigate the individual object. As mentioned earlier there is possibility that these objects are co-moving system or false positive. This is determined with careful consideration of separation, Parallax, proper angle and the binding energy to determine if the system is bound or not. The criteria for the binding energy for the Multiple star system is different from that of the binary system. Hence, the value of the absolute binding energy cannot be used for the determination of a possible multiple star system.

### 2.5.1 J0112-7031

J0112-7013 with RA and DEC 18.09239 and  $-70.52291$  is found have J0112-7031A as its companion. The separation between these objects is  $2.32 \times 10^4 AU$  with  $|U_g| = 1.901 \times 10^{35} J$ . The binding energy of the system is sufficient to meet the criteria to be bound system[4]. Aladin image search found 2MASS J0112216-703123 to be the closest match with this object on simbad directory. The spectral type of the objects are considered to be M7-L8 UCD(Ultracool dwarfs)[19][20]. 2MASS J0112216-703123 is classified as M7 type[20] which shows that system is still very young. This object is a considered to be a strong candidate for binary system.

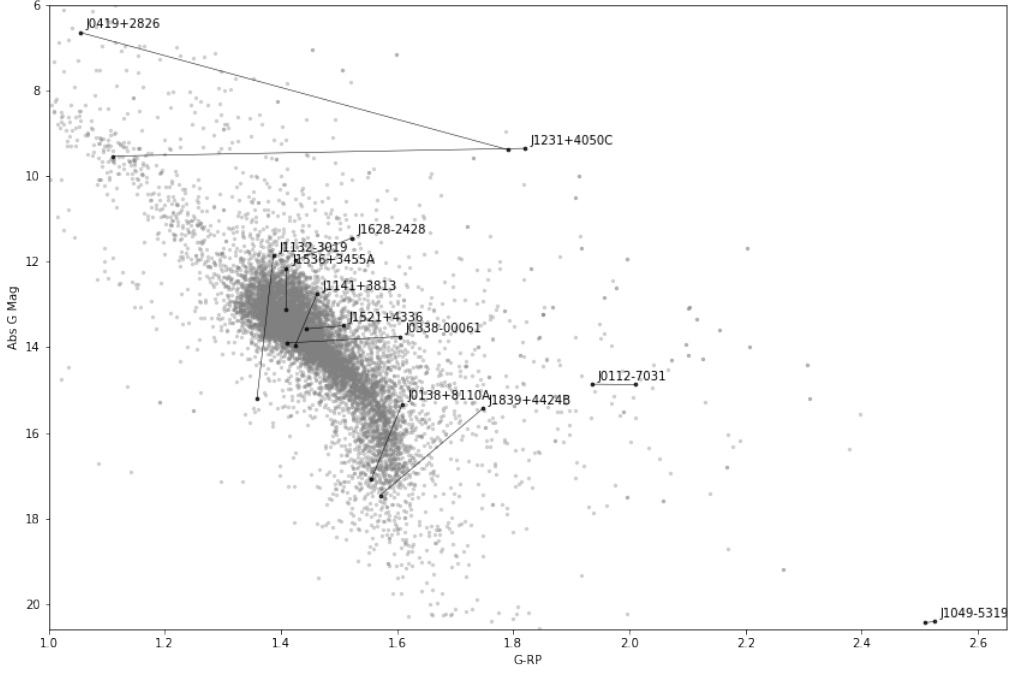


Figure 2.7: Binary systems that do not show typical behaviour and hence are interesting to study as part of this investigation. The objects are either too far, or have very similar absolute magnitude or at different stage of star life than expected.

### 2.5.2 J0138+8110A

J0138+8110A with RA and DEC 24.787510 and 81.166582 is found have J0138+8110B as its companion. This is first mentioned with GAIA DR2 in 2018. It is classified as Brown dwarf candidate[17]. The separation between these objects is  $2.18 \times 10^5 au$  with binding energy of  $-2.019 \times 10^{34} J$ . The binding energy of the system is sufficient to meet the criteria for a bound system[4]. The difference in the parallax is  $\approx 0.6 mas$  which is within the  $3\sigma$ . This system is considered as a qualifying candidate for binary system.

### 2.5.3 J0338-00061

J0338-00061 with RA and DEC 54.683183 and  $-0.115057$  is found have J0338-0006 as its companion. The close reference to this is found as 2MASS J03384389-0006541 in Simbad with references as part of the GAIA and SDSS data investigation for the general trend. The object is classified as M7V [21] as part of the spectrometric M dwarfs in SDSS 7th data release. Its companion is found to be close match to SDSS J033842.64-000612.9, which is M6V in the SDSS DR7 [21]. The spectrometric value suggests that this is fairly young system. The separation between these objects is  $3.58 \times 10^5 au$  with binding energy of  $1.2311 \times 10^{33} J > 10^{33} J$  limit hence considered as bound system. The proper motion of these two objects is very similar with  $\delta PM_{RA} = 1.59 mas/yr$  and  $\delta PM_{dec} = -0.7 mas/yr$ . The proper motion, parallax and the After careful consideration of the separation and binding energy this system is not considered to be a qualified as binary candidate.

### 2.5.4 J0419+2826

J0419+2826 with RA and DEC 64.859489 and 28.437181 is found have J0419+2827 as its companion. This is also known as WK811, a Tau type star with spectral type K7. Its companion has a close match with V\* FR Tau, which is a variable star with spectral type M5.3. The separation between these objects is  $5.80 \times 10^4 au$  with binding energy of  $7.605 \times 10^{33} J$  which is more than the binding energy limit[4] is considered as bound system. The proper motion difference  $\delta PM_{RA} = 3.7 mas/yr$  and  $\delta PM_{dec} = -0.5 mas/yr$ . The values of binding energy and the separation mentioned in table 2.1, this is consider candidate for binary system.

### 2.5.5 J1049-5319

J1049-5319 with RA and DEC 162.30843 and  $-53.31806$  is found have J1049-5319B as its companion. The separation between these objects is  $0.184au$  with binding energy of  $2.391 \times 10^{39}J$ . The binding energy of the system is high which can be explained considering the small separation. The separation and the location on HR diagram of this system are the main reasons to investigate it.

The object  $J1049 - 5319$  is also known as *Luhman16* [22], which is well known binary system with small separation. Several investigations have been done by to investigate the characteristics and the spectrum of the objects. This object is described as L7.5 brown dwarf system. This is certainly interesting for further investigation but beyond the nature of this investigation. As sufficient evidence is available to show that the object is well known object hence no further investigation is requires at this point for the binary of the object.

### 2.5.6 J1132-3019

J1132-3019 with RA and DEC 173.075840 and  $-30.331184$  is found have J1132-3018 as its companion. The primary is also known as TWA 30A and the companion is known as TWA30B. The system is investigated by several astronomers and is defined as obscured binary in recent publication [23]. The separation between these objects is  $1.53 \times 10^4au$  with binding energy of  $2.877 \times 10^{34}J$ . The binding energy of the system is sufficient to meet the criteria to be binary system[4]. The separation and the binding energy meet the criteria for these systems to be define as binary at initial level. In publication in *A&A* April 2021[23] this system is observed using NACO, IFS and IRDIS with different filters. This object is considered as binary system based on the previous publications and the binding energy values.

### 2.5.7 J1141+3813

J1141+3813 with RA and DEC 175.343950 and  $38.218050$  is found have J1141+3820 as its companion. The primary object is also known as SDSS J114122.58+381305.5, while the companion is SDSS J114131.05+382055.0. The separation between these objects is  $6.31 \times 10^5au$  with binding energy of  $6.992 \times 10^{32}J$ . The spectral class of both objects are M7V[21] from the SDSS DR7. The binding energy of the system is smaller than the  $|U_g|$  empirical limit and hence this system is considered to be an unbound system. The proper motion difference  $\delta PM_{RA} = 0.16mas/yr$  and  $\delta PM_{dec} = 5.9mas/yr$ . This is probable a co-moving system.

### 2.5.8 J1231+4050C

J1231+4050C with RA and DEC 188.056980 and  $41.045884$  is found have J1231+4050B as its companion. Although there is known system found near the primary while the secondary object is found to be 2MASS J12321930+4101107 is High proper motion star. Considering the nearby objects this may be the part of the co-moving system or a triple or quadruple system with J1231+4050 and J1231+4050A. The separation between these objects is  $9.515 \times 10^3au$  with binding energy of  $-4.634 \times 10^{34}J$ . The binding energy suggests that the object is bound with sufficient separation to be qualify as the binary systems. Need further observations to be able to make certain conclusion.

### 2.5.9 J1521+4336

J1521+4336 with RA and DEC 230.478090 and  $43.608819$  is found have J1521+4336A as its companion. This object suggested to be 2MASS J15215482+4336318. The object have the photometric reference it to be a M8V type object[21]. The separation between these objects is  $6.21 \times 10^4au$  with binding energy of  $7.096 \times 10^{33}J$ . The  $|U_g|$  value of this system just above the minimum absolute energy of bound system. The proper motion difference  $\delta PM_{RA} = 0.4mas/yr$  and  $\delta PM_{dec} = 0.6mas/yr$ . Considering the other criteria and the fact that the binding energies in table 2.1 are approximate values, this will be considered for the further investigation.

### 2.5.10 J1536+3455A

J1536+3455A with RA and DEC 234.227350 and  $34.929176$  is found have J1536+3455 as its companion. The closet objects that matched with this object in simbad database, for primary is

LP 273-45 and secondary is LP 273-46. These are high proper motion stars. The spectral type of the secondary is M6V, while no spectral value of primary is not published on simbad. The proper motion of these object is very close to each other. The separation between these objects is  $1.65 \times 10^4 au$  with binding energy of  $2.667 \times 10^{34} J$ . The separation and the binding energy of the system satisfy the criteria to be considered as bound system.

### 2.5.11 J1628-2428

J1628-2428 with RA and DEC 247.075370 and  $-24.476770$  is found have J1628-24281 as its companion. The simbad reference of this object is found to be BKL T J162818-242836 and secondary is BKL T J162847-242814. Both of the objects are defined as M6D type[24]. The separation between these objects is  $1.23 \times 10^5 au$  with binding energy of  $3.575 \times 10^{33} J$ . The absolute value of the binding energy of the system is slightly higher than the limiting value. The proper motion difference  $\delta PM_{RA} = 3.3 mas/yr$  and  $\delta PM_{dec} = 2.6 mas/yr$ . Considering the separation, proper motion and the binding energy this system satisfy the criterion to be a bound system.

### 2.5.12 J1839+4424B

J1839+4424B with RA and DEC 279.871770 and 44.411473 is found have J1839+4424A as its companion. The primary object in simabad has reference 2MASS J18392917+4424386 and secondary object 2MASS J18392735+4424484. The spectrum of the primary is defined to be M8.9V while no information on the spectrum is published for the secondary object. The parallax difference between the objects is  $0.001 mas$ , which is very small. The proper motion difference  $\delta PM_{RA} = 9.2 mas/yr$  and  $\delta PM_{dec} = 2.01 mas/yr$ . Which suggest a higher difference in the proper motion. The separation between these objects is  $1.61 \times 10^4 au$  with  $|U_g| = 2.732 \times 10^{34} J$ . The absolute binding energy satisfies the empirical limit and hence is considered for the mass approximation to calculate a more appropriate value of the binding energy.

## Chapter 3

# Evaluation

These systems satisfy all conditions including separation, proper motion difference, parallax difference and position angle. Further these also have binding energy  $|U_g| > 2.5 \times 10^{33} \text{J}$  and the found to be isochrones within the error limits. The initial conditions chosen for the processing of the data are quite strict in order to rule out the detection of false binary systems. The processing of data provides us a useful information about these systems as mentioned in table 2.5.

### 3.1 Known and Unknown Binary Systems

Interpretation of the information with reliability and accuracy is very important. In order to understand the nature of the unknown binary systems it is important to understand the nature of the known binary system. The known binary systems provide us information about the expected nature of the binaries. This could also help us to classify then in different type of binaries based on the properties.

The comparison of the percentage of the known binaries and the proportion of the number of unknown binaries selected using them as benchmark shows consistency in results. The percentage is found to be 9.03% and 7.6% for known binaries and unknown binaries respectively. About distribution of binaries this tells us that less than 10% of the binary systems are quite young with ages  $< 0.1$  Gyrs.

The age of the known binaries can be used to calculate the empirical isochrones. These can be use to calculate the more accurate ages and the masses of the binary systems. The ages of the isochrones are quite close to their expected ages. The in figure 2.4 and 2.5, the isochrones crosses each other. ATMO(BACH15) isochrones are defined the evolutionary track of low mass stars. These low mass stars are also binaries. Without these set of the known and unknown binaries it would be difficult to explain the reason of it. Upon observing the nature of the binaries in figure 2.4 and 2.5 and considering the fact that the binary systems are isochrones. The nature of the binaries close to the intersection of isochrones approximately at  $G-K = 7$  and  $\text{Abs G Mag} = 17.8$ , the binaries lies close or on the these isochrones shows similar behaviour. In order to explain the reason for unexpected behaviour of these binaries and isochrones investigation of the physical properties is required. These physical properties may include the atmospheric properties and the composition of the binary system.

### 3.2 Idp fraction values of binary system

The GAIA data provide us a lot of new information. one of the similar feature is `idp_frac_multi_peak`. This provide us the ipd fraction for the multiple peak. The higher the value the higher the probability of the system to be binary system. The fraction is provided as percentage. If the value of `idp_frac_multi_peak`  $> 50$ , the object could be a binary system.

The `idp_frac_multi_peak`  $> 0$  is only present for 12.74% of the objects used for this research project and 0.7% have `idp_frac_multi_peak`  $> 50$ . The percentage of the objects that are in the list of known binaries is only 11.6%. It is 10% for the binary systems that are considered as benchmark. which is is one out of 10 object have `idp_frac_multi_peak`  $> 50$ . The histogram of the distribution of `idp_frac_multi_peak` is shown in figure 3.1(left).

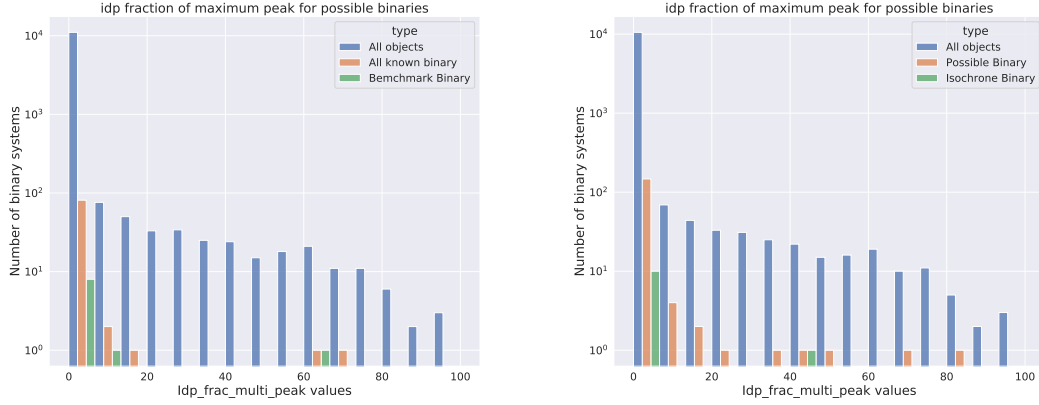


Figure 3.1: Above histogram shows the number of the primary objects of the (left) known binary systems and (Right)possible(prospective)binary systems with different `idp_frac_multi_peak`. This shows the distribution of the values of the idp fraction as percentage. In both cases the known binary systems and the binaries that are possible candidates for the binary systems, the numbers of the objects with idp fraction value greater than 50 is very small.

Considering the fact that very small amount of the objects have `idp_frac_multi_peak` value provided in the data. the low percentage of the object with idp peak value for the objects detected as binary from other surveys provide us evidence that the valued for the idp. Th possible explanation for this low value of `idp_frac_multi_peak` values for known binary systems could be due to the quality of observations taken. Due to the lack of good data for idp multipeak fraction value in GAIA DR3, it is not used for investigation. Hopefully, next release of data GAIA DR4 will provide us more information.

### 3.3 New binary systems

During the processing of the data the 11 systems were selected as the isochrones mentioned in the table 2.3. The system J0433+1810 have two companions but only one of it is isochrone. This could be because J0433+1758 is just a false companion of it or it is a co-moving star. Which require the calculation of the binding energy of the system. Considering the fact it could be the triple system, hence it is not considered at this point in the list of the binary system. Hence the final list of the binary selection for the further investigation is in the table 3.1.

Star_A	Mass_A( $M_{\odot}$ )	Star_B	Mass_B( $M_{\odot}$ )	$ U_g(J) $
J0003-1040A	0.055	J0003-1040	0.04	9.538570e+31
J0008-0851A	0.2	J0008-0851	0.055	5.522677e+32
J0856+3746A	0.6	J0856+3746B	0.13	8.506270e+31
J0109-5100A	0.35	J0109-5100	0.02	4.357892e+32
J0112-7031	0.15	J0112-7031A	0.15	1.710913e+34
J0032+6714A	0.3	J0032+6714B	0.03	1.133690e+34
J1112+3548A	1.1	J1112+3548	0.015	1.448038e+33
J0414+2648	0.35	J0414+2646	0.35	1.392551e+34
J0003-2822A	1.0	J0003-2822	0.2	1.296337e+35
J0419+2826	0.4	J0419+2827	0.06	7.300400e+33

Table 3.1: The objects that are considered for the final list of the object as this satisfy all the conditions. As J0433+1810 could be the triple system. Hence this is not considered for the further investigation at this point. Hence, 10 out of 11 is considered for the investigation. Base on the estimated mass the absolute energy of the binding energy of the systems is calculated.

The absolute binding energy( $|U_g|$ ) of the systems is calculated using the estimated mass. This

will help us to differentiate between the objects with enough binding energy[4] for the system to be in a bound system. Out of the 10 objects, 5 objects match the criteria for the binding energy with  $|U_g| > 2.5 \times 10^{33} J$ [4]. This produces the list of the object that satisfy all of the criteria that are theoretically essential to be a binary system. Although the binding energy criteria is a bit flexible depends on the type of the system.

The table 3.2 provided us the final list of the binary objects. These objects can be individually investigate in order to remove the error of detecting a false binary.

Star_A	Mass_A( $M_\odot$ )	Star_B	Mass_B( $M_\odot$ )	$ U_g(J) $
J0112-7031	0.15	J0112-7031A	0.15	1.710913e+34
J0032+6714A	0.3	J0032+6714B	0.03	1.133690e+34
J0414+2648	0.35	J0414+2646	0.35	1.392551e+34
J0003-2822A	1.0	J0003-2822	0.2	1.296337e+35
J0419+2826	0.4	J0419+2827	0.06	7.300400e+33

Table 3.2: This is the final list of the binaries that satisfy all conditions. The objects satisfy the initial conditions of separation, proper motion and parallax difference. These are also found to be isochrones and also have absolute binding energy greater then the minimum energy required [4]

The list of these objects can be use to identify the further properties such as spectrum to identify the characteristics of these binary systems.

### 3.4 Strange Objects

The objects with the strange nature possesses the knowledge to improve our understanding about the universe. These challenges our understanding of current universe. In order to explain the strange nature of these objects, it is important to carefully consider the object to investigate as binary. As to classify them as binary they must have to have enough binding energy to be considered as bound system. Some of these strange objects are provided in table 3.3

<i>StarA</i>	<i>Spectrum</i>	<i>StarB</i>	<i>separation</i>	$ U_g (J)$
J0112 – 7031	M7	J0112 – 7031A	2319.746	1.09e + 35
J0138 + 8110A	-	J0138 + 8110B	21844.149	2.019e + 34
J0419 + 2826	K7	J0419 + 2827	57989.658	7.605e + 33
J1132 – 3019	M0.75[23]	J1132 – 3018	15329.97	2.877e + 34
J1521 + 4336	M8V	1521 + 4336A	62143.459	7.096e + 33
J1536 + 3455A	-	J1536 + 34551	6533.303	2.667e + 34
J1628 – 2428	M6D	J1628 – 24281	123337.242	3.575e + 33
J1839 + 4424B	M8.9V	J1839+4424A	16141.268	2.732e + 34

Table 3.3: Primary and secondary object with possible classification and spectral values.

Although these objects are interesting to be investigated further. In order to investigate these it is important to consider the binaries with similar behaviours in the list of known binaries. This will provide us an insight in the understanding the cause of such an unusual behaviour. Which may require further observation of these objects from the ground based telescopes or the data related to these objects from other surveys. As these can provide us the vital information such as spectrometry.

In figure 3.2 shows the distribution of these strange objects on the colour magnitude diagram showing their expected age and the mass. This also shoes that the objects are not isochrones as expected nature of the binary systems. This require further data in order to be able to understand the reason for these objects to behave in this way. which is beyond the scope of this projects. Although the future release of GAIA DR4 data and the comparison of the data from other surveys could provide us more information.

This would not be ideal to do any further investigation of these objects without understanding the nature of the strange binary systems in the list of the known binaries.



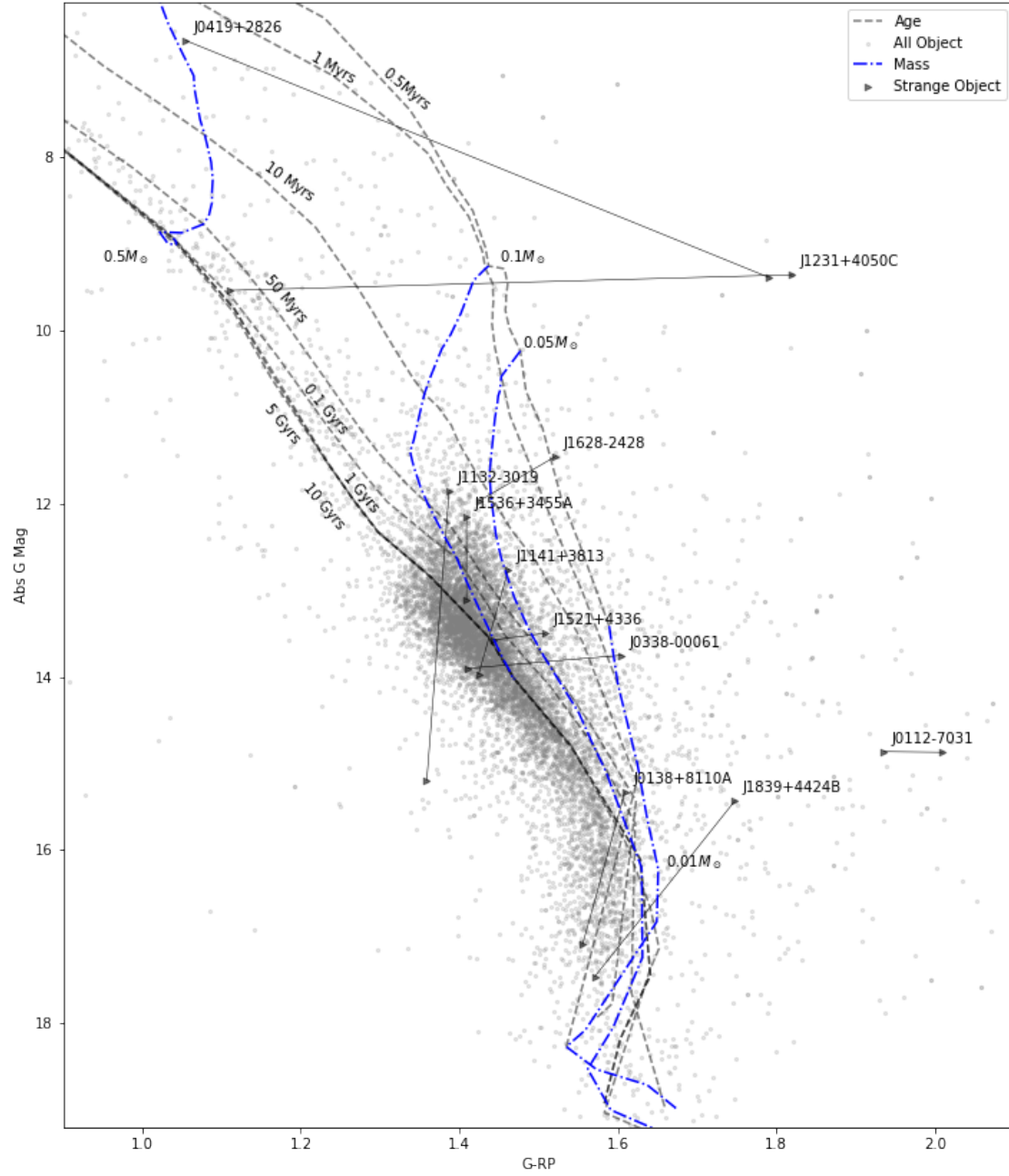


Figure 3.2: Binary candidates with isochronic fitting from ATMOs(BACH15). Black line represent the ages and blue line represent the mass of the objects in solar masses  $M_{\odot}$

## Chapter 4

# Conclusion and Future plans

### 4.1 Conclusion

The "Master\_withDR3.csv" contains 14279 sources from the Gaia EDR3 and from other surveys such as SDSS and 2MASS. 11369 objects are found to be in the Gaia EDR3. All of the parameters of these 11369 objects from EDR3 are stored in new dataset. Some of these objects do not have parallax value and hence the number of objects available for the investigation is 10702. Therefore, 25.05% of the data is found to be not useful leaving 74.95% of useful data.

Using the conditions mentioned earlier in section 2.1, the binary systems were detected from the 10702 Gaia EDR3 data. The total number of the detected objects using the algorithm are 228. After this, the best approach was to use the `idp_frac_multi_peak` to filter out the objects that have value greater than 50, which could filter out the objects that have 2 peaks in the data detected by CCDs. The 0.7% of the data contain `idp_frac_multi_peak` value which could not provide significant information. It could be used during later investigation, `idp_frac_multi_peak` may contain more information in full DR3.

84 out of 228 binary systems are found to be in the known systems and 142 are possible candidate for new binary systems. After careful consideration of the error in the absolute G magnitude and the error in G-K magnitude error from empirical binary systems, 11 objects were found to lie parallel to the isochrones from ATMO(BAHC15) model. This provides us the estimated mass of these binary systems used for the calculation of the absolute binding energy. In these 11 binary systems, J0433+1810 is a triple system with J0433+1758 and J0433+1750 as its companion. This is found by the algorithm in section 2.1. In this triple system, J0433+1750 is isochrone to the primary; J0433+1758 does not have similar age as its primary. This object was taken out from the list of prospective binaries, as triple systems are beyond the scope of this project.

The system which meets all of the above criteria can only be classified as binary system if it is a bound system. If the system is not a bound system, it cannot revolve about a common centre of mass. The absolute binding energy for the rest of the 10 objects is calculated using the mass from ATMO(BACH15) model. Only 5 of these 10 objects satisfy the condition  $|U_g| > 2.5 \times 10^3 \text{J}$  [4]. This produces the list of the final 5 objects which can be investigated to understand their properties and the type of the binary systems.

The systems in the table 3.2 can be classified as binaries as they satisfy all conditions to be a binary system. Further investigation and cross-matching with the data from other surveys will provide us more information about the properties of these systems.

### 4.2 Future Plans

In this investigation, 5 objects are found to be the binary systems. Their properties are still to be investigated. The DR3 full release will provide more parameters including photometry and spectroscopy data. The `idp_frac_multi_peak` will also help to classify the resolved and unresolved binaries.

During this project, we also encountered some objects that show unusual behaviours. Some of them are unknown binaries and the others are also in known binaries. These systems need to be investigated in order to understand the reason for their unusual behaviour. The data provided in the Gaia EDR3 can be compared with the data from the previous surveys to improve our understanding

of the systems that are classified as binaries in the previous surveys. This comparison of the data can also be used to validate the binarity of these strange systems, which can help to explain the systems in table 2.1.

The mass and the age of the systems are estimated using the theoretical isochrones model. There will always be a degree of error while simulating the evolution of a star. ATMO(BAHC15) model is chosen because this model includes masses as small as  $0.01M_{\odot}$ . The stars with age greater than 0.1 Gyrs were very close to each other, therefore the isochrones of these stars overlapped. This makes it difficult to predict the mass and the age of the systems whose age is greater than 1.0 Gyrs. This could be resolved using empirical isochrones and the age of white dwarfs to predict the age of the companions of white dwarfs. This will also provide the reference to predict the age of empirical isochrones. This will make it possible to search for more systems with age greater than 0.1 Gyrs.

This investigation is based on a small portion of the Gaia EDR3 data. The same algorithm can be used to detect other binary systems in the complete Gaia EDR3 dataset, as this will provide us a wider range of the known binary systems to produce more accurate empirical isochrones. The machine learning could be used to predict the equation of an isochrone line and hence the distance between the object and the line. This distance could be used to predict the age more accurately. This will also help us to understand the nature of the binary systems with the help of new properties described in Gaia only such as `idp_fraction_multi_peak`. Combining the model developed in this project with machine learning will not only help to identify new binary systems but also validate the previously known binary systems.



# Appendix A

## Preview of Master\_withDR3.csv

```
In [1]: import pandas as pd
data = pd.read_csv("Master_withDR3.csv")
pd.set_option("display.max_columns", None) # setting to show all columns
print(data.head(5)) # displaying top 5 rows of files
```

	SHORTNAME	DISCOVERYNAME	DISCOVERYREFNAME	RA	\
0	J0000+1523	ULASJ000005.87+152354.4	2016A&A...589A..49S	0.024492	
1	J0000+1136	ULASJ000010.43+113602.2	2015MNRAS.450.2486C	0.043463	
2	J0000+2554	2MASS00001354+2554180	2004AJ...127.3553K	0.056354	
3	J0000+0051	...	2008AJ...135..785W	0.091531	
4	J0000-1245	2MASSJ0000286-124515	2007AJ...133..439C	0.118741	

	DEC	POSITIONREFNAME	POSITIONEPOCH	PECULIARNAME	\
0	15.398469	2007MNRAS.379.1599L	2007.82	...	
1	11.600600	2007MNRAS.379.1599L	2010.57	...	
2	25.905569	2006AJ...131.1163S	2016.00	...	
3	0.858103	GDR3	2016.00	...	
4	-12.754698	GDR3	2016.00	...	

	PECULIARREFNAME	MGCANDIDACYNAME	MGCANDIDACYREFNAME	MULTIPLEFLAGNAM	\
0	...	...	CHI:2.2200000		
...					
1	...	...	...		
...					
2	...	...	...		
...					
3	...	...	...		
...					
4	...	...	...		
...					

	MULTIPLEFLAGREFNAME	COMMENTSNAME	SPTOPTNAME	\
0	...	companionGD22772085696588395776?	...	
1	...	...	T1.5:	
2	...	...	...	
3	...	...	M6	
4	...	...	M8.5	

	SPTOPTREFNAME	SPTNIRNAME	SPTNIRREFNAME	SPTPHONAME	\
0	...	...	...	L2:	
1	SIMBAD	...	...	T1.5:	
2	...	T4.5	2006ApJ...639.1095B	...	
3	2008AJ...135..785W	...	...	...	
4	2007AJ...133..439C	M9	2014ApJ...794..143B	...	

	SPTPHOREFNAME	SPTNUM	PARALLAX	PARALLAXERR	\
0	2016A&A...589A..49S	72.0	-99999.00000	-99999.000000	
1	2015MNRAS.450.2486C	81.5	-99999.00000	-99999.000000	
2	...	84.5	70.80000	1.900000	
3	...	66.0	3.13702	0.626729	
4	...	68.5	30.26870	0.406703	

	PARALLAXREFNAME	PMRA	PMRAERR	PMDEC	PMDECERR	\
0	...	-99999.0000	-99999.000000	-99999.0000	-99999.000000	
1	...	-99999.0000	-99999.000000	-99999.0000	-99999.000000	
2	2012ApJS...201...19D	-19.0900	1.207690	126.6700	1.297980	
3	GDR3	55.1722	0.916306	29.0686	0.327195	
4	GDR3	-142.7220	0.382480	-104.6820	0.407190	

	PMREFNAME	RV	RVERR	RVREFNAME	TMASSJ	\
0	...	-99999.0	-99999.0	...	16.925	

1	.....	-99999.0	-99999.0	.....	18.650	
2	2012ApJS..201...19D	-99999.0	-99999.0	.....	15.063	
3	2018A&A...616A...1G	-99999.0	-99999.0	...	16.353	
4	2018A&A...616A...1G	-99999.0	-99999.0	...	13.200	

	TMASSJERR	TMASSH	TMASSHERR	TMASSK	TMASSKERR	TMASSFLAGNAME	\
0	0.197	15.789	0.197	15.879	0.262	...	
1	0.080	-99999.000	-99999.000	-99999.000	-99999.000	...	
2	0.041	14.731	0.074	14.836	0.120	AAB	
3	0.105	15.741	0.138	15.406	0.179	ABC	
4	0.026	12.445	0.023	11.973	0.023	AAA	

	WISEW1	WISEW1ERR	WISEW2	WISEW2ERR	WISEW3	WISEW3ERR	WISEFLAGNAME	\
0	-99999.0	-99999.0	-99999.0	-99999.0	-99999.0	-99999.0	...	
1	-99999.0	-99999.0	-99999.0	-99999.0	-99999.0	-99999.0	...	
2	-99999.0	-99999.0	-99999.0	-99999.0	-99999.0	-99999.0	...	
3	-99999.0	-99999.0	-99999.0	-99999.0	-99999.0	-99999.0	...	
4	-99999.0	-99999.0	-99999.0	-99999.0	-99999.0	-99999.0	...	

	PS1G	PS1GERR	PS1R	PS1RERR	PS1I	PS1IERR	\
0	-99999.0	-99999.0	-99999.0000	-99999.0000	-99999.0000	-99999.0000	
1	-99999.0	-99999.0	-99999.0000	-99999.0000	-99999.0000	-99999.0000	
2	-99999.0	-99999.0	-99999.0000	-99999.0000	-99999.0000	-99999.0000	
3	-99999.0	-99999.0	21.1428	0.1638	21.9649	0.2451	
4	-99999.0	-99999.0	-99999.0000	-99999.0000	-99999.0000	-99999.0000	

	PS1Z	PS1ZERR	PS1Y	PS1YERR	PS1FLAGNAME	\
0	-99999.0000	-99999.0000	-99999.0000	-99999.0000	...	
1	-99999.0000	-99999.0000	-99999.0000	-99999.0000	...	
2	19.1681	0.0126	17.4245	0.0096	52	
3	-99999.0000	-99999.0000	-99999.0000	-99999.0000	36	
4	-99999.0000	-99999.0000	-99999.0000	-99999.0000	...	

SI	\	PS1REFNAME	SDSSG	SDSSGERR	SDSSR	SDSSRERR	SDS
0		...	-99999.000	-99999.000	-99999.000	-99999.000	-99999.0
00							
1		...	-99999.000	-99999.000	-99999.000	-99999.000	-99999.0
00							
2		2016arXiv161205242M	26.173	0.546	24.025	0.613	23.3
52							
3		2016arXiv161205242M	-99999.000	-99999.000	-99999.000	-99999.000	-99999.0
00							
4		...	-99999.000	-99999.000	-99999.000	-99999.000	-99999.0
00							

	SDSSIERR	SDSSZ	SDSSZERR	SDSSFLAGNAME	SDSSREFNAME	\
0	-99999.000	-99999.000	-99999.000	...	...	
1	-99999.000	-99999.000	-99999.000	...	...	
2	0.597	18.409	0.036	281543964623104	2000AJ....120.1579Y	
3	-99999.000	-99999.000	-99999.000	...	...	
4	-99999.000	-99999.000	-99999.000	...	...	

	IRACCH1	IRACCH1ERR	IRACCH2	IRACCH2ERR	MKOY	MKOYERR	\
0	-99999.0	-99999.0	-99999.0	-99999.0	18.4653	0.044784	
1	-99999.0	-99999.0	-99999.0	-99999.0	-99999.0000	-99999.000000	
2	-99999.0	-99999.0	-99999.0	-99999.0	-99999.0000	-99999.000000	
3	-99999.0	-99999.0	-99999.0	-99999.0	-99999.0000	-99999.000000	
4	-99999.0	-99999.0	-99999.0	-99999.0	-99999.0000	-99999.000000	

	MKOJ	MKOJERR	MKOH	MKOHERR	MKOK	\
0	17.2745	0.027014	16.506	0.027793	15.9155	
1	-99999.0000	-99999.000000	-99999.000	-99999.000000	-99999.0000	

```

2      14.8451      0.005453      14.730      0.070000 -99999.0000
3 -99999.0000 -99999.000000 -99999.000 -99999.000000 -99999.0000
4 -99999.0000 -99999.000000 -99999.000 -99999.000000 -99999.0000

      MKOKERR      MKOREFNAME      GAIAG      GAIAGERR      GAIABP \
0      0.026358 2007MNRAS.379.1599L 22.3411 -99999.000000 20.7354
1 -99999.000000 ... 24.6440 -99999.000000 22.7401
2 -99999.000000 2007MNRAS.379.1599L 21.3803 0.031821 NaN
3 -99999.000000 ... 19.7478 0.003939 21.3422
4 -99999.000000 ... 17.7528 0.001791 20.8356

      GAIABPERR      GAIARP      GAIARPERR      GAIATOG      GAIAREFNAME      RA2000 \
0 -99999.000000 21.7247 -99999.000000 0 ... 0.024492
1 -99999.000000 23.3441 -99999.000000 0 ... 0.043463
2 NaN 19.6446 0.140626 0 ... 0.056429
3 0.130517 18.3684 0.021565 3 GDR3 0.091285
4 0.175280 16.1707 0.004779 3 GDR3 0.119383

      DEC2000      SIMBADNAME      SIMBADTYPENAME      SIMBADRADVEL \
0 15.398469 ... -99999.0
1 11.600600 ULASJ000010.43+113602.2 brownD* NaN
2 25.904998 2MASSJ00001354+2554180 brownD* NaN
3 0.857974 SDSSJ000021.91+005128.8 low-mass* 15.0
4 -12.754235 DENISJ000028.6-124514 low-mass* NaN

      SIMBADSPNAME      SPTOPT      SPTNIR      SPTPHO      BINSEP      SOURCE_ID_OBJID \
0 ... -99999.0 -99999.0 72.0 -99999.0 0
1 T1.5: -99999.0 -99999.0 81.5 -99999.0 0
2 T4.5 -99999.0 84.5 -99999.0 -99999.0 0
3 M7V 66.0 -99999.0 -99999.0 -99999.0 2738307526856177152
4 M9.2V 68.5 69.0 -99999.0 -99999.0 2421137424841635840

      SOURCE_ID_DR2_OBJID      SPTGEN      TYPEFLAGNAME      SPECQUALITYNAME      JGEN \
0 0 72.0 ... p 16.925
1 0 81.5 ... p 18.650
2 0 84.5 ... i 15.063
3 2738307526856177152 66.0 ... o 16.353
4 2421137424841635840 68.5 ... o 13.200

      VTAN      EVTAN      DMOD      GAIASEP      RA2016      DEC20
16 \
0 -99999.00000 -99999.000000 -99999.000000 -99999.000000 0.024492 15.3985
00
1 -99999.00000 -99999.000000 -99999.000000 -99999.000000 0.043463 11.6006
00
2 8.57621 0.258957 -0.749834 -99999.000000 0.056335 25.9056
00
3 94.22760 18.882600 -7.517420 0.000263 0.091530 0.8581
03
4 27.71730 0.382558 -2.595030 0.002047 0.118733 -12.7547
00

      LITPARALLAX      LITPARALLAXERR      LITPARALLAXREFNAME
0 -99999.0 -99999.0 .....
1 -99999.0 -99999.0 .....
2 70.8 1.9 2012ApJS...201...19D
3 -99999.0 -99999.0 ...
4 -99999.0 -99999.0 ...

```

In [ ]:

## Appendix B

# List of known binary systems used for cross-matching

This is a preview of the data from the list of known binaries compiled by Prof.R.Smart. This list is used for the detection of known binary system from the list of systems detected by the algorithm.

```
In [2]: import pandas as pd
data = pd.read_csv("/home/alok/Documents/GAIAproject/DATA/basicinfo.csv")
pd.set_option("display.max_columns", None) # setting to show all columns
data.head(10) # displaying top 5 rows of files
```

```
Out[2]:
```

	ShortnameS	NameS	RAS_d	DeS_d	SpTSname	NameP	RAp_d	Dep_d	SpTPname	EpochPos	Refname	Sep
0	J0000+05_3	000000.8+054802.57	0.003423	5.800713	M1	0000+0547	0.001853	5.797406	K7	-9999.0	2015AJ.....150...57D	13.17
1	J0000+15	000000.9+151501.65	0.003820	15.250460	K2	0000+1515	0.004429	15.251429	M1	-9999.0	2015AJ.....150...57D	4.08
2	J0000-02	000001.4-020434.51	0.005757	-2.076252	M2	0000-0204	0.004689	-2.075740	M2	-9999.0	2015AJ.....150...57D	4.26
3	J0000+04_2	000001.4+045902.34	0.005923	4.983983	M2	0000+0459	0.003491	4.985660	M2	-9999.0	2015AJ.....150...57D	10.61
4	J0000+21	000002.7+213758.17	0.011139	21.632826	M0	0000+2138	0.009783	21.636292	K4	-9999.0	2015AJ.....150...57D	13.28
5	J0000+06_5	000002.7+065514.87	0.011184	6.920798	M1	0000+0655	0.011619	6.920529	M1	-9999.0	2015AJ.....150...57D	1.83
6	J0000+31	000003.1+314916.57	0.012792	31.821268	M2	0000+3149	0.013974	31.818804	M1	-9999.0	2015AJ.....150...57D	9.58
7	J0000+30_1	000003.2+301551.64	0.013474	30.264345	M3	0000+3015	0.013625	30.264977	M3	-9999.0	2015AJ.....150...57D	2.32
8	J0000+06_2	000003.5+063704.93	0.014557	6.618035	M6	0000+0637	0.013983	6.617012	M0	-9999.0	2015AJ.....150...57D	4.22
9	J0000+10_3	000003.9+105518.34	0.016052	10.921762	M2	0000+1055	0.017086	10.921094	M2	-9999.0	2015AJ.....150...57D	4.38

```
In [ ]:
```



# Appendix C

## Python Code

The jupyter notebooks used to write code for this project can be found on github. <https://github.com/as-uh/MSc-data-Science-project/tree/main/code>

The code for the algorithm used to detect the binary systems is shown below

```
In [11]: primary_companions = {}
for i in range(len(matched_data)):
    obj1 = matched_data.iloc[i]['SHORTNAME']
    obj2 = Converttolist(matched_data.iloc[i]['COMPANIONS'])
    obj2.append(obj1) #merging matched objects together
    all_obj = remove_duplicate(obj2)

    ra = matched_data.iloc[i]['RA'] #Right Ascension
    dec = matched_data.iloc[i]['DEC'] # Declination
    radius= 1.
    filter = data['RA'] > (ra - radius/np.cos(dec*np.pi/180))
    filter &= data['RA'] < (ra + radius/np.cos(dec*np.pi/180))
    filter &= data['DEC'] > (dec - radius)
    filter &= data['DEC'] < (dec + radius)
    data_filtered = data[filter]
    obj_dict={}
    for j in range(len(data_filtered)):
        if data_filtered.iloc[j]['SHORTNAME'].strip() in all_obj:
            obj_dict[data_filtered.iloc[j]['SHORTNAME'].strip()] = (
                data_filtered.iloc[j]['GAIA'] +
                5*np.log10(data_filtered.iloc[j]['PARALLAX']/100.))
    brightest_obj = min(obj_dict.items(), key = lambda x : x[1])
    obj2.remove(brightest_obj[0])
    primary_companions[brightest_obj[0]] = obj2

dict_new={}
key_rm=[]
for i in primary_companions:
    for j in primary_companions:
        if i==j:
            continue
        if primary_companions[i] == primary_companions[j]:
            dict_new[
                '\n'.join(map(
                    str, primary_companions[i]))] = [i,j]
            key_rm.append(i)
            key_rm.append(j)

keys_to_remove = set(key_rm).intersection(
    set(primary_companions.keys()))
for key in keys_to_remove:
    del primary_companions[key]
primary_companions.update(dict_new)

primary_final=[]
secondary_final=[]

for keys,values in primary_companions.items():
    primary_final.append(keys)
    for value in values:
        secondary_final.append(value)

primary_table=[]
for i in range(len(data)):
    if data.iloc[i]['SHORTNAME'].strip() in primary_final:
        primary_table.append(data.iloc[i,:].values)

primary_table = pd.DataFrame(primary_table, columns = column_names)
```

# Bibliography

- [1] F Marocco, R L Smart, E E Mamajek, L M Sarro, A J Burgasser, J A Caballero, J M Rees, D Caselden, K L Cruz, R Van Linge, and et al. The gaia ultra-cool dwarf sample – iii: seven new multiple systems containing at least one gaia dr2 ultracool dwarf. *Monthly Notices of the Royal Astronomical Society*, 494(4):4891–4906, Apr 2020.
- [2] D. Hobbs, L. Lindegren, U. Bastian, S. Klioner, A. Butkevich, C. Stephenson, J. Hernandez, U. Lammers, A. Bombrun, F. Mignard, M. Altmann, M. Davidson, J. de Bruijne, J. Fernández-Hernández, H. Siddiqui, and E. Utrilla. Gaia EDR3 documentation Chapter 4: Astrometric data. Gaia EDR3 documentation, March 2021.
- [3] G. Busso, C. Cacciari, M. Bellazzini, J. M. Carrasco, F. De Angeli, D. W. Evans, C. Fabricius, C. Jordi, P. Montegriffo, E. Pancino, M. Rainer, and N. Sanna. Gaia EDR3 documentation Chapter 5: Photometric data. Gaia EDR3 documentation, March 2021.
- [4] J. A. Caballero. Reaching the boundary between stellar kinematic groups and very wide binaries. *Astronomy Astrophysics*, 507(1):251–259, Sep 2009.
- [5] F. van Leeuwen, J. de Bruijne, C. Babusiaux, J. Castañeda, D. Hobbs, G. Busso, P. Sartoretti, E. Utrilla, X. Luri, P. M. Marrese, A. Mora, C. Fabricius, J. González-Núñez, N. Hambly, G. Altavilla, M. Altmann, T. Antoja, F. Arenou, J. Bakker, E. Balbinot, C. Barache, U. Bastian, N. Bauchet, M. Bellazzini, M. Biermann, R. Blomme, A. Bombrun, A. Brown, D. Busonero, A. Butkevich, C. Cacciari, J. M. Carrasco, N. Cheek, M. Clotet, O. Creevey, C. Crowley, H. Cánovas, M. David, M. Davidson, F. De Angeli, S. Diakité, R. Drimmel, J. Duran, D. W. Evans, M. Fabrizio, J. Fernández-Hernández, F. Figueras, K. Findeisen, A. Garcia-Gutierrez, Gracia-Abril. G., R. Guerra, R. Gutiérrez-Sánchez, A. Helmi, M. Henar Sarmiento, J. Hernandez, A. Hutton, C. Jordi, S. Khanna, S. Klioner, U. Lammers, N. Leclerc, L. Lindegren, W. Löffler, S. Marinoni, J. Martín-Fleitas, E. Masana, A. Masip Vela, A. Masip, R. Messineo, D. Michalik, F. Mignard, P. Montegriffo, T. Muraveva, K. Nienartowicz, E. Pancino, C. Panem, J. Portell, E. Racero, M. Rainer, P. Ramos, C. Reylé, C. Ríos Diaz, A. Riva, A. Robin, A. Robin, T. Roegiers, M. Romero-Gómez, N. Rowell, J. Rybizki, J. Salgado, N. Sanna, G. Seabroke, J. C. Segovia, H. Siddiqui, R. Smart, C. Stephenson, D. Teyssier, F. Torra, C. Turon, J. Valero, A. Vallenari, M. van Leeuwen, and M. Weiler. Gaia EDR3 documentation. Gaia EDR3 documentation, March 2021.
- [6] C. Babusiaux, E. Masana, A. Robin, F. Arenou, C. Reylé, and P. Sartoretti. Gaia EDR3 documentation Chapter 2: Simulated data. Gaia EDR3 documentation, March 2021.
- [7] J. Castañeda, D. Hobbs, C. Fabricius, M. Davidson, N. Rowell, L. Lindegren, N. Hambly, U. Bastian, J. Portell, F. Torra, M. Clotet, R. Smart, A. Mora, M. Biermann, W. Löffler, A. Brown, D. Busonero, and A. Riva. Gaia EDR3 documentation Chapter 3: Pre-processing. Gaia EDR3 documentation, March 2021.
- [8] R. L. Smart, F. Marocco, L. M. Sarro, D. Barrado, J. C. Beamín, J. A. Caballero, and H. R. A. Jones. The Gaia ultracool dwarf sample - II. Structure at the end of the main sequence. , 485(3):4423–4440, May 2019.
- [9] Niall R. Deacon, Michael C. Liu, Eugene A. Magnier, Kimberly M. Aller, William M. J. Best, Trent Dupuy, Brendan P. Bowler, Andrew W. Mann, Joshua A. Redstone, William S. Burgett, Kenneth C. Chambers, Peter W. Draper, H. Flewelling, Klaus W. Hodapp, Nick Kaiser, Rolf Peter Kudritzki, Jeff S. Morgan, Nigel Metcalfe, Paul A. Price, John L. Tonry, and Richard J.

Wainscoat. Wide Cool and Ultracool Companions to Nearby Stars from Pan-STARRS 1. , 792(2):119, September 2014.

- [10] F. M. Jiménez-Esteban, E. Solano, and C. Rodrigo. A catalog of wide binary and multiple systems of bright stars from gaia-DR2 and the virtual observatory. *The Astronomical Journal*, 157(2):78, jan 2019.
- [11] Jieun Choi, Aaron Dotter, Charlie Conroy, Matteo Cantiello, Bill Paxton, and Benjamin D. Johnson. Mesa Isochrones and Stellar Tracks (MIST). I. Solar-scaled Models. , 823(2):102, June 2016.
- [12] F. Spada, P. Demarque, Y.-C. Kim, T. S. Boyajian, and J. M. Brewer. The yale-potsdam stellar isochrones. *The Astrophysical Journal*, 838(2):161, apr 2017.
- [13] Alessandro Bressan, Paola Marigo, Léo Girardi, Bernardo Salasnich, Claudia Dal Cero, Stefano Rubele, and Ambra Nanni. parsec: stellar tracks and isochrones with the padova and trieste stellar evolution code. *Monthly Notices of the Royal Astronomical Society*, 427(1):127–145, Oct 2012.
- [14] Sebastian L. Hidalgo, Adriano Pietrinferni, Santi Cassisi, Maurizio Salaris, Alessio Mucciarelli, Alessandro Savino, Antonio Aparicio, Victor Silva Aguirre, and Kuldeep Verma. The updated BaSTI stellar evolution models and isochrones. i. solar-scaled calculations. *The Astrophysical Journal*, 856(2):125, mar 2018.
- [15] Garrett Somers, Lyra Cao, and Marc H. Pinsonneault. The spots models: A grid of theoretical stellar evolution tracks and isochrones for testing the effects of starspots on structure and colors. *The Astrophysical Journal*, 891(1):29, Mar 2020.
- [16] I. Baraffe, D. Homeier, F. Allard, and G. Chabrier. New evolutionary models for pre-main sequence and main sequence low-mass stars down to the hydrogen-burning limit. , 577:A42, May 2015.
- [17] Reyl , C. New ultra-cool and brown dwarf candidates in gaia dr2. *AA*, 619:L8, 2018.
- [18] Kareem El-Badry, Hans-Walter Rix, Yuan-Sen Ting, Daniel R. Weisz, Maria Bergemann, Phillip Cargile, Charlie Conroy, and Anna-Christina Eilers. Signatures of unresolved binaries in stellar spectra: implications for spectral fitting. *Monthly Notices of the Royal Astronomical Society*, 473(4):5043–5049, 10 2017.
- [19] J. Davy Kirkpatrick, Dagny L. Looper, Adam J. Burgasser, Steven D. Schurr, Roc M. Cutri, Michael C. Cushing, Kelle L. Cruz, Anne C. Sweet, Gillian R. Knapp, Travis S. Barman, John J. Bochanski, Thomas L. Roellig, Ian S. McLean, Mark R. McGovern, and Emily L. Rice. DISCOVERIES FROM a NEAR-INFRARED PROPER MOTION SURVEY USING MULTI-EPOCH TWO MICRON ALL-SKY SURVEY DATA. *The Astrophysical Journal Supplement Series*, 190(1):100–146, aug 2010.
- [20] Kelle L. Cruz, I. Neill Reid, J. Davy Kirkpatrick, Adam J. Burgasser, James Liebert, Adam R. Solomon, Sarah J. Schmidt, Peter R. Allen, Suzanne L. Hawley, and Kevin R. Covey. Meeting the cool neighbors. IX. the luminosity function of m7-l8 ultracool dwarfs in the field. *The Astronomical Journal*, 133(2):439–467, jan 2007.
- [21] Andrew A. West, Dylan P. Morgan, John J. Bochanski, Jan Marie Andersen, Keaton J. Bell, Adam F. Kowalski, James R. A. Davenport, Suzanne L. Hawley, Sarah J. Schmidt, David Bernat, Eric J. Hilton, Philip Muirhead, Kevin R. Covey, B rbara Rojas-Ayala, Everett Schlawin, Mary Gooding, Kyle Schluns, Saurav Dhital, J. Sebastian Pineda, and David O. Jones. THE SLOAN DIGITAL SKY SURVEY DATA RELEASE 7 SPECTROSCOPIC m DWARF CATALOG. i. DATA. *The Astronomical Journal*, 141(3):97, feb 2011.
- [22] K. L. Luhman. DISCOVERY OF a BINARY BROWN DWARF AT 2 pc FROM THE SUN. *The Astrophysical Journal*, 767(1):L1, mar 2013.

- [23] V Christiaens, M-G Ubeira-Gabellini, H Cánovas, P Delorme, B Pairet, O Absil, S Casassus, J H Girard, A Zurlo, Y Aoyama, G-D Marleau, L Spina, N van der Marel, L Cieza, G Lodato, S Pérez, C Pinte, D J Price, and M Reggiani. A faint companion around CrA-9: protoplanet or obscured binary? *Monthly Notices of the Royal Astronomical Society*, 502(4):6117–6139, 02 2021.
- [24] Catherine L. Slesnick, Lynne A. Hillenbrand, and John M. Carpenter. A large-area search for low-mass objects in upper scorpius. II. age and mass distributions. *The Astrophysical Journal*, 688(1):377–397, nov 2008.